JACS
JOURNAL OF THE AMERICAN CHEMICAL SOCIETY
Article
pubs.acs.org/JACS

Iron(II) Complexes Containing Unsymmetrical P−N−P′ Pincer Ligands for the Catalytic Asymmetric Hydrogenation of Ketones and Imines

Paraskevi O. Lagaditis, Peter E. Sues, Jessica F. Sonnenberg, Kai Yang Wan, Alan J. Lough, and Robert H. Morris*

Department of Chemistry, University of Toronto, 80 St. George Street, Toronto, Ontario M5S 3H6 Canada

Supporting Information

ABSTRACT: After their treatment with $LiAlH_4$ and then alcohol, new iron dicarbonyl complexes *mer-trans*-[Fe(Br)-$(CO)_2$(P−CH═N−P′)][BF_4] (where P−CH═N−P′ = R_2PCH_2CH═$NCH_2CH_2PPh_2$ and R = Cy or *i*Pr or P−CH═N−P′ = (*S*,*S*)- Cy_2PCH_2CH═$NCH(Me)CH(Ph)$-PPh_2) are catalysts for the hydrogenation of ketones in THF solvent with added KO*t*Bu at 50 °C and 5 atm H_2. Complexes with R = Ph are not active. With the enantiopure complex, alcohols are produced with an enantiomeric excess of up to 85% (*S*) at TOF up to 2000 h^{-1}, TON of up to 5000, for a range of ketones. An activated imine is hydrogenated to the amine in 90% ee at a TOF 20 $h^{-1}$and TON 99. This is a significant advance in asymmetric pressure hydrogenation using iron. The complexes are prepared in two steps: (1) a one-pot reaction of phosphonium dimers ([*cyclo*-$(PR_2CH_2CH(OH)^-)_2$][$Br]_2$), KO*t*Bu, $FeBr_2$, and $Ph_2PCH_2CH_2NH_2$ (or (*S*,*S*)-$Ph_2PCH(Ph)CH$-$(Me)NH_2$ for the enantiopure complex) in THF under a CO atmosphere to produce the complexes *cis*- and *trans*-[$Fe(Br)_2$(CO)(P−CH═N−P′)]; (2) the reaction of these with $AgBF_4$ under CO(g) to afford the dicarbonyl complexes in high yield (50−90%). NMR and DFT studies of the process of precatalyst activation show that the dicarbonyl complexes are converted first to hydride−aluminum hydride complexes where the imine of the P−CH═N−P′ ligand is reduced to an amide [P−CH_2N−P′]$^-$ with aluminum hydrides still bound to the nitrogen. These hydride species react with alcohol to give monohydride amine iron compounds FeH(OR′)(CO)(P−CH_2NH−P′), R′ = Me, CMe_2Et as well as the iron(0) complex $Fe(CO)_2$(P−CH_2NH−P′) under certain conditions.

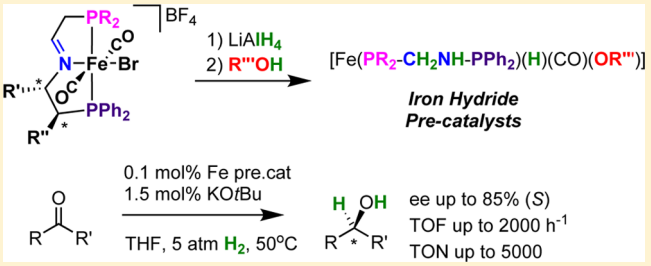

INTRODUCTION

Current research in the field of catalytic hydrogenation has moved toward developing complexes that do not employ platinum group metals such as Ir, Rh, or Ru.[1] These platinum group metals are expensive because of their low abundance and are toxic; hence, they are undesirable for some applications. Several examples of catalysts based on 3d metals have appeared in the literature in recent years that have been shown to be competitive with these precious metal-based catalysts for the asymmetric catalytic reduction of unsaturated bonds.[2−11] Some systems based on enzymes,[12−15] and metal-free compounds are also promising.[16−22]

In recent years, a variety of iron-based hydrogenation catalysts have been developed because iron is abundant, cheap, and nontoxic.[23−27] Our group reported that an iron compound with a tetradentate ligand was moderately active for the asymmetric hydrogenation of acetophenone under basic conditions with a turnover frequency (TOF) of 5 h^{-1} resulting in an enantiomeric excess (ee) of 27% (*S*) toward 1-phenylethanol (**M1** of Figure 1). We found that the monocarbonyl derivative of **M1** was a good asymmetric transfer hydrogenation precatalyst for ketones at room temperature,[28] and later Beller and co-workers showed that it also worked for activated imines.[29] Since then we have focused on optimizing the transfer hydrogenation catalysts and have developed highly active and enantioselective iron(II) catalysts, [Fe(P−N−N−P)(CO)(Br)][BPh_4], where P−N−N−P is a unique tetradentate ligand, (*S*,*S*)-$Ph_2PCH_2CHNC(H)PhC(H)$-$PhNCHCH_2PPh_2$ formed by the condensation of an (*S*,*S*)-diamine with phosphine aldehydes templated by iron(II).[30,31] We have also modified the ligand by substituting the phenyl substituents on phosphorus with alkyl or substituted phenyl substituents to examine their effects on the catalytic behavior.[32,33] The precatalysts are activated *in situ* by reaction with base (KO*t*Bu) to form bis-eneamido iron(II) complexes which are then subsequently half reduced by isopropanol.[34,35] The catalytic reduction of ketones involves a bifunctional mechanism where the ligand is directly involved in the catalysis.[35,36] Our catalysts are exceedingly efficient for the reduction of prochiral ketones by transfer of hydrogen from isopropanol achieving TOFs of up to 200 s^{-1}, conversions of

Received: August 13, 2013

   dx.doi.org/10.1021/ja4082233 | J. Am. Chem. Soc. XXXX, XXX, XXX−XXX

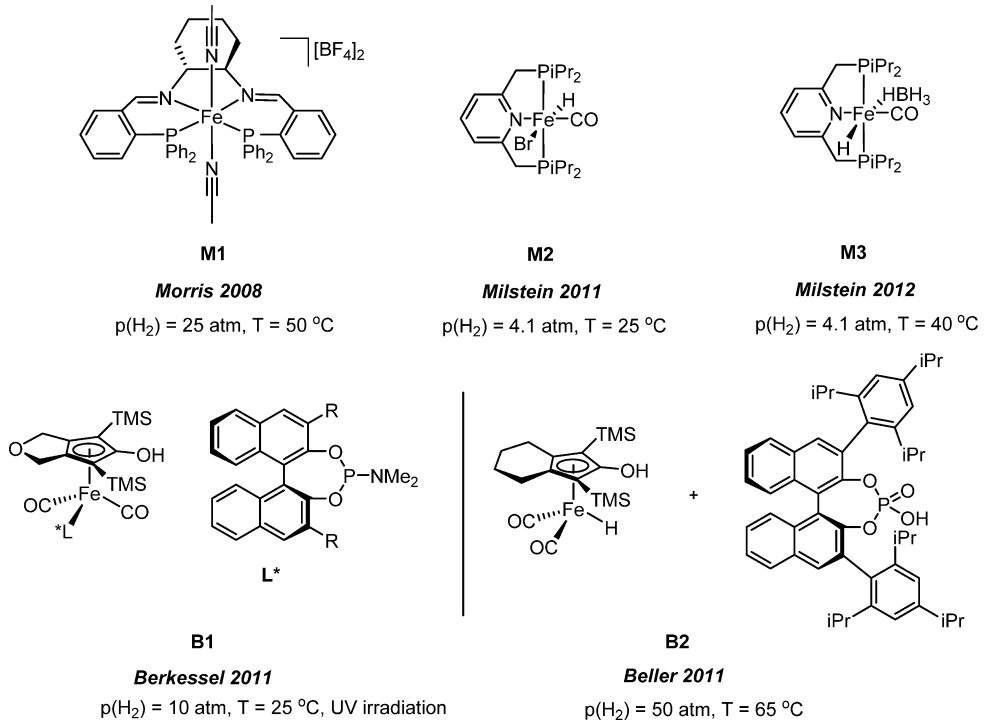

Figure 1. Active iron catalysts for ketone (**M1**−**3** and **B1**) and imine (**B2**) hydrogenation.

99%, with enantioselectivity (ee) toward one enantiomer of the alcohol as high as 98% at room temperature.[35,37] They are also active and exceptionally enantioselective for the transfer hydrogenation of certain activated imines.[37,38] Transfer hydrogenation of ketones in this way is an equilibrium process, and sometimes racemization of the product alcohol is observed. Therefore, we sought an active asymmetric catalyst that utilizes H_2 gas, thereby enabling the irreversible hydrogenation of substrates in order to conveniently achieve complete conversion without racemization of the product alcohol.

Recent work by Milstein and co-workers demonstrated that tridentate P−N−P pincer ligands can be effective. Their iron(II) complexes, Fe{2,6-(P*i*Pr$_2$CH$_2$)$_2$C$_5$H$_3$N}(H)(CO)(Br) (**M2**)[39] and Fe{2,6-P*i*Pr$_2$CH$_2$)$_2$C$_5$H$_3$N}(H)(CO)(HBH$_3$) (**M3**)[40] shown in Figure 1, were found to be active for the catalytic hydrogenation of ketones with 4.1 atm H_2, achieving turnover numbers (TON) for acetophenone hydrogenation of up to 1720 with TOF of approximately 430 h^{-1} at 40 °C for **M2** and up to 1980 with TOF 300 h^{-1} at 40 °C for **M3**. The latter complex did not require activation by the addition of base. A mechanistic investigation using experimental and DFT methods led to the conclusion that the catalysts operate by Milstein's well-established aromatization−dearomatization of the P−N−P ligand that has been previously demonstrated to occur with Ru analogues.[41−43] More recently, Kirchner and co-workers have presented an analogue to **M1**, Fe{2,6-(P*i*Pr$_2$CH$_2$)$_2$C$_5$H$_3$N}(H)(CO)(Cl) with −NH in place of the methylene linkers between the pyridine and phosphorus groups on the P−N−P ligand. The have also observed dearomatization and aromatization under hydrogen; however, no report of catalytic activity in hydrogenation of ketones was reported.[44] In the current work we generate asymmetric catalysts related to these using our templated ligand synthesis methodology.

Knölker's Fe(II) complex was found by Casey and co-workers to catalyze the hydrogenation of ketones via a bifunctional mechanism using H_2 gas under mild conditions.[45−48] More recently Berkessel et al. synthesized a chiral analogue of Knölker's complex by the replacement of a CO ligand with chiral phosphoramidite ligands (**B1**, Figure 1),[49] while Beller and co-workers added a chiral phosphoric acid as a cocatalyst (**B2**, Figure 1).[50,51] The Berkessel system hydrogenated acetophenone under UV irradiation with 10 atm H_2 at 25 °C with nine turnovers in 24 h to give 1-phenylethanol in 30% ee, while the Beller system produced chiral amines in up to 96% ee using 50 atm H_2 and 65 °C with 16 turnovers based on iron in 24 h. Herein we report our progress toward discovering more active iron(II) catalysts for the asymmetric H_2 hydrogenation of polar bonds.

RESULTS AND DISCUSSION

Template Synthesis of Iron(II) Complexes. We previously reported the synthesis of the iron(II)−P−CH═N−P′ complexes, [Fe(Ph$_2$PCH$_2$CH$_2$N═CHCH$_2$PR$_2$)-(NCCH$_3$)$_3$]$^{2+}$ (where R = Ph or Cy), by means of a multicomponent template synthesis using a cyclic phosphonium salt as a source of phosphine-aldehyde, [Fe(H$_2$O)$_6$]-[BF$_4$]$_2$, KO*t*Bu, and 2-(diphenylphosphino)ethylamine in acetonitrile.[52] These P−CH═N−P′-pincer ligands have inequivalent phosphorus donors, a feature which is not easy to achieve by the conventional means of synthesis of P−N−P-pincer ligands.[53−55] The ^{31}P{^{1}H} NMR spectra of both complexes displayed two AB doublets with a large $^2J_{PP}$ coupling of 160 Hz for R = Ph and 148 Hz for R = Cy, indicating that the P are *trans*; this indicates a *mer*-arrangement of the P−CH═N−P′ ligand about iron.

With this strategy in mind, we modified our template synthesis procedure and used FeBr$_2$ as our iron source. Initially we conducted the reaction shown in Scheme 1 in THF under a N_2 atm in hopes of isolating an Fe(P−CH═N−P′)(Br)$_2$ complex; however, no reaction occurred. Upon exposure of the reaction mixture to carbon monoxide, the pale-yellow slurry

dx.doi.org/10.1021/ja4082233 | J. Am. Chem. Soc. XXXX, XXX, XXX−XXX

Scheme 1. Template Synthesis of Iron Complexes, *trans*-[Fe(P−CH═N−P′)(CO)$_2$(Br)][BF$_4$]

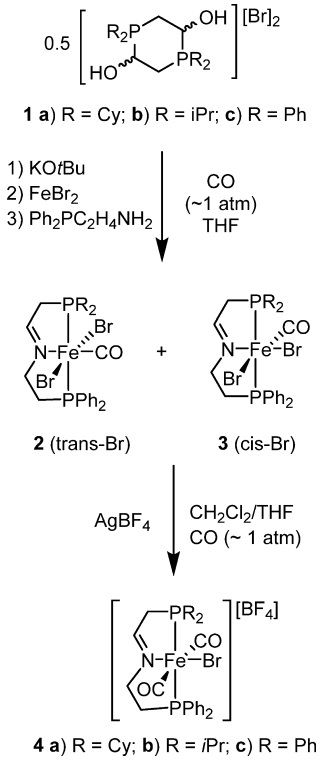

immediately turned red-purple. After stirring for sufficient time (5 h) and removal of salts (KBr and excess $FeBr_2$) a red-purple solid was isolated. Starting with the phosphonium dimer **1a** with R = Cy, iron compounds were produced in approximately a 1:1 ratio based on the $^{31}P\{^1H\}$ NMR spectra. One set of doublets was observed at 67.8 and 71.9 ppm ($^2J_{PP}$ = 172 Hz) and a second set at 39.6 and 60.5 ppm ($^2J_{PP}$ = 201 Hz). The large coupling constants are indicative that the P atoms of the P−CH═N−P′ ligand are *trans* about the iron metal center. Similar results were obtained from **1b** with R = *i*Pr and **1c** with R = Ph (Table S1 in Supporting Material [SI]). Hence, two isomers of iron complexes formed: trans-Br (**2a-c**) and cis-Br (**3a-c**) (Scheme 1). The formation according to Scheme 1 of two *mer*-Fe(P−CH═N−P′)(CO)(Br)$_2$ isomers contrasts with Milstein's system where only the *trans* Br isomer was isolated.[39]

Our results closely resemble those of Kirchner and co-workers who have developed the synthesis of Fe(P−N−P)(CO)(X)$_2$ complexes, where X is Cl or Br, based on the pincer ligand, 2,6-(P*i*Pr$_2$NH)$_2$C$_5$H$_3$N.[56,57] They have found that when X is Cl the cis isomer formed under solvent-free conditions while the trans isomer formed in solution. However, in the case where X is Br, they did not observe the same selectivity and always obtained a mixture of cis and trans isomers. We attempted to make the Cl analogue as well using the Cl salt of **1b** and $FeCl_2$ in the template synthesis but both cis and trans isomers formed as well based on the $^{31}P\{^1H\}$ NMR spectrum of the reaction mixture (see the SI, Table S1). We postulate that in our case there is no control of *cis*- and *trans*-Br or -Cl isomers since we are employing a multi-component reaction where the ligand is made *in situ*.

We tested the compound Fe(CO)$_4$(Br)$_2$[58] as a starting iron source, reasoning that, if the halides are already coordinated to iron and the CO ligands are removed under UV light, we could selectively form one isomer. When Fe(CO)$_4$(Br)$_2$ was used in place of $FeBr_2$, there was an immediate release of gas as well as a color change to orange. A $^{31}P\{^1H\}$ NMR spectrum of this mixture revealed an intractable mixture. This was then exposed to UV light. After at least 5 h, the solution turned dark purple and a $^{31}P\{^1H\}$ NMR spectrum of the solid isolated upon workup showed that the isomer at 67.8 and 71.9 ppm ($^2J_{PP}$ = 175 Hz) (R = Cy) was the major species with, on average, less than 10% of other species. Crystals suitable for X-ray crystallography were isolated and confirmed selective formation of the *trans*-Fe(Cy$_2$PCH$_2$CH═NCH$_2$CH$_2$PPh$_2$)(CO)(Br)$_2$ complex, **2a** (Figure 2). Complex *trans*-Fe(*i*Pr$_2$PCH$_2$CH═NCH$_2$CH$_2$PPh$_2$)(CO)(Br)$_2$, **2b**, using phosphonium dimer **1b** was also made in this manner. However, in the case of phosphonium dimer **1c**, a mixture of *cis*- and *trans*-isomers, **2c** and **3c**, formed in every attempt. These photochemical syntheses have several limitations such as low yields and the formation of *cis*-[Fe(P−CH═N−P′)(CO)$_2$(Br)]$^+$ as described in the SI and thus were not pursued further.

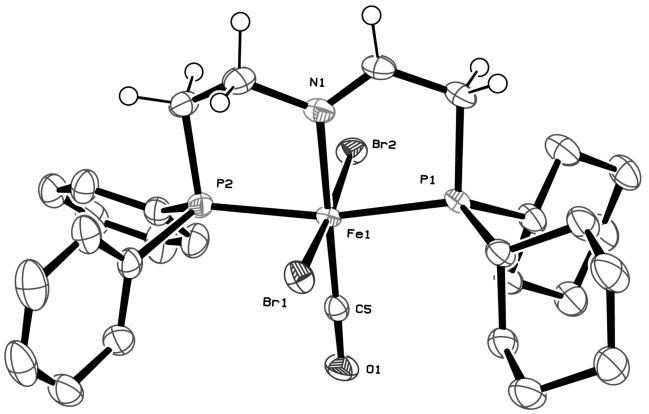

Figure 2. ORTEP plot (thermal ellipsoids at 30% probability) of the X-ray crystal structure of *trans*-Fe(Cy$_2$PCH$_2$CH═NCH$_2$CH$_2$PPh$_2$)(CO)(Br)$_2$, **2a**. Hydrogen atoms of Ph and Cy substituents removed for clarity. Selected bond lengths (Å) and angles (deg): Fe(1)−P(1): 2.2680(9); Fe(1)−P(2): 2.2613(9); Fe(1)−N(1): 2.011(2); Fe(1)−Br(1): 2.4545(5); N(1)−C(2): 1.269(4); N(1)−C(3): 1.479(4): O(1)−C(5): 1.138(4); C(5)−Fe(1)−N(1): 177.6(1); P(2)−Fe(1)−P(1): 167.75(3); Br(1)−Fe(1)−Br(2): 175.12(2).

Kirchner and co-workers have reported the formation of *trans*-[Fe(P−N−P)(CO)$_2$(Br)][BF$_4$] compounds selectively from the reaction of a halide abstractor (such as $AgBF_4$) with a mixture of *cis*- and *trans*-Fe(P−N−P)(CO)(Br)$_2$ isomers.[59] Hence, upon inclusion of $AgBF_4$ in our procedure there was an immediate color change from red-purple to bright purple, the color of complexes **4a−c** (Scheme 1). The $^{31}P\{^1H\}$ NMR spectra of isolated compounds showed the formation of one new iron complex with AB doublets with smaller $^2J_{PP}$ couplings of 82 Hz (R = Cy), 85 Hz (R = *i*Pr) and 94.5 Hz (R = Ph), significantly smaller than that of *cis*-[Fe(P−CH═N−P′)(CO)$_2$(Br)]$^+$ with $^2J_{PP}$ = 145 Hz (see the SI). Crystals of **4a** and **4b** suitable for X-ray crystallography were obtained (Figure 3) and confirmed that the *trans*-CO geometry about iron also occurred with our compounds. We believe the mechanism for this selective *trans* configuration follows the one proposed by Kirchner and co-workers because we also found that this reaction can occur in the absence of carbon monoxide;[59] however, to achieve high yields (85−90%) we conducted the halide abstraction step under one atmosphere of CO. The

dx.doi.org/10.1021/ja4082233 | J. Am. Chem. Soc. XXXX, XXX, XXX−XXX

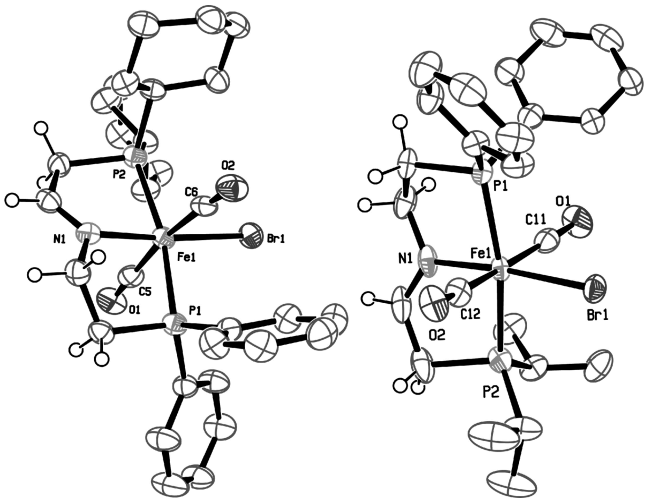

Figure 3. ORTEP plot (thermal ellipsoids at 30% probability) of the X-ray crystal structures of **4a** (left) and **4b** (right). The BPh_4^- anions of **4a**, the BF_4^- anions of **4b** and hydrogen atoms of Ph, Cy and *i*Pr substituents removed for clarity. Selected bond lengths (Å) and angles (deg) of **4a**: Fe(1)−C(6): 1.829(4); Fe(1)−N(1): 1.980(3); Fe(1)−P(2): 2.271(1); Fe(1)−Br(1): 2.4416(6); O(1)−C(5): 1.104(4); O(2)−C(6): 1.132(4); N(1)−C(3): 1.275(5); N(1)−C(2): 1.482(4); C(6)−Fe(1)−C(5): 172.2(2); P(2)−Fe(1)−P(1): 168.38(4); N(1)−Fe(1)−Br(1): 175.35(9); and of **4b**: Fe(1)−P(1): 2.265(2); Fe(1)−N(1): 1.980(4); Fe(1)−C(12): 1.803(6); Br(1)−Fe(1): 2.4530(8); O(2)−C(12): 1.144(6); N(1)−C(2): 1.270(6); N(1)−C(3): 1.477(7); C(12)−Fe(1)−C(11): 170.4(2); P(1)−Fe(1)−P(2): 167.40(5); N(1)−Fe(1)−Br(1): 174.9(1).

$^{13}C\{^1H\}$ NMR spectra of complexes **4a−c** displayed only one broad triplet or a doublet of doublets (dd) for the CO ligands at approximately 210 ppm which indicates that the complexes have the expected C_s symmetry. The ^{13}CO analogue of **4b** (henceforth referred to as **4b-^{13}CO**) was synthesized to further confirm via NMR spectroscopy that two CO ligands are coordinated to iron. The $^{31}P\{^1H\}$ NMR (CD_2Cl_2) spectrum of **4b-^{13}CO** displayed the same two phosphorus resonances as **4b** at 45.5 and 78.3 ppm ($^2J_{PP}$ = 86 Hz, $^2J_{PC}$ = 22 Hz) but with a triplet of doublet multiplicity instead of a doublet for each phosphorus atom. The $^{13}C\{^1H\}$ NMR spectrum of **4b-^{13}CO** displayed one intense CO triplet resonance at 211.7 ppm ($^2J_{CP}$ = 24 Hz).

The chiral aminophosphine, (*S*,*S*)-2-amino-1-phenylpropyl-diphenylphosphine was successfully used in the template synthesis method to generate the chiral complex, (*S*,*S*)-**4d** (Scheme 2). (*S*,*S*)-**4d** was designed with Cy substituents on the ligand in anticipation that the bulky groups would enhance enantiomeric interactions with the substrate during catalysis. The $^{13}C\{^1H\}$ NMR spectrum of (*S*,*S*)-**4d** showed two inequivalent CO resonances with a dd pattern at 210.5 and 214.7 ppm. The IR spectra of complexes **4a−d** displayed only one ν_{CO} absorption in the range from 2000 to 2011 cm^{-1}, similar to those of the *trans*-CO iron complexes reported by Kirchner and coworkers.

Scheme 2. Synthesis of the chiral iron complex, (*S*,*S*)-[Fe(P−CH═N−P′)(CO)$_2$(Br)][BF$_4$], (*S*,*S*)-4d

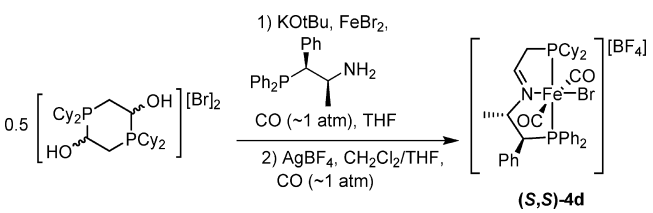

Catalytic Hydrogenation. The discovery of the activation of the precatalysts **4a−d** for hydrogenation was made while treating these well-defined iron dicarbonyl complexes with various hydride reagents. The objective was to produce iron hydride amine complexes with the bifunctional HN-FeH group known to efficiently reduce C═O and C═N bonds.[23,35,37] Reactions with $NaHBEt_3$ or $NaBH_4$ resulted in the formation of intractable mixtures. The use of $LiAlH_4$ was more promising. To generate iron hydrides, often a precursor is reacted with a slight excess of $LiAlH_4$ in THF,[60−64] sometimes with the addition of a protic solvent.[65−69] In the present case, we found that the addition of at least 6 equiv of $LiAlH_4$ was necessary to produce a solution of iron hydride complexes reproducibly (see below). The mixture was then treated with alcohol until gas evolution had ceased. Methanol, ethanol, and *tert*-amyl alcohol (2-methyl-2-butanol, *t*AmylOH) were found to give active catalyst preparations. Then the ketone or imine substrate and additional THF were added, and the entire solution was injected into a prepared pressure reactor. This procedure then allowed facile and efficient screening of optimal conditions for catalysis (Table 1).

It was discovered that, while 25 atm H_2 was an effective pressure for catalysis, the use of 5 atm still resulted in full conversion of acetophenone to 1-phenylethanol within 15 min. Unsurprisingly, faster conversions were observed at 50 °C than at 25 °C (Table 1, entry 2 vs 3). Substitution of $LiAlH_4$ with $NaAlH_4$ did not affect the rate of reaction (entry 4). No catalysis was observed in the absence of base (entry 7) which prevents the testing of base-sensitive substrates. The use of a tertiary alcohol, *t*AmylOH, in the catalyst activation process was observed to create a more active system than the primary alcohols, MeOH or ethanol (entry 2 vs 5 vs 6). There are at least two possible explanations for this alcohol effect; either the catalyst activation period could be slower with methoxide or ethoxide as a ligand, or there are other deactivation processes that are more pronounced with a primary alkoxide.[70] The use of a tertiary alcohol also has the advantage of preventing a nonselective transfer hydrogenation mediated by $Al(OR)_3$. It appears to be imperative for the P−N−P′ ligand to contain at least one large alkyl-substituted phosphorus atom to create an active catalyst (Table 1, entries 1 and 2 vs 9). We do not yet know whether this is a steric or electronic effect and at which stage in catalysis it applies. The TOF value for the hydrogenation of acetophenone using the **4a** precatalyst (entry 8, TON 2000, TOF 1980 h^{-1} at 50 °C and 5 atm H_2) is comparable to that reported for Milstein's complexes **M2**, 430 h^{-1} at 40 °C, 4 atm H_2. A difference of the present system is that THF can be used in place of the alcohol solvent needed for catalysis with **M2** or **M3** of Figure 1.

In the case of the hydrogenation of benzaldehyde, it was found that the higher pressure of 10 atm of H_2 gas was needed to achieve 90% conversion in 2.5 h vs 10 h with 5 atm H_2 gas (Scheme 3).

Finally, the substrate scope of the asymmetric hydrogenation reaction of ketones was investigated with the conditions of 50 °C and pressure of 5 atm H_2 using 0.1 mol % of the activated mixture prepared from (*S*,*S*)-**4d** (Table 2). Many of the aryl ketones were converted to the alcohols with good enantioselectivity, typically about 80% (*S*). This system represents a

dx.doi.org/10.1021/ja4082233 | J. Am. Chem. Soc. XXXX, XXX, XXX−XXX

Table 1. Hydrogenation of Acetophenone Catalyzed by Achiral Complexes 4a,b Once Activated by Reaction with $LiAlH_4$ and Then Alcohol[a]

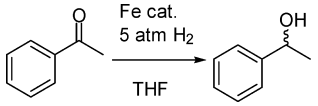

entry	precatalyst[a]	base[b]	temp. (°C)	alcohol[a]	C/S ratio	time (min, 99% conv)	TOF[c] (h^{-1})
1	**4a**	KO*t*Bu	50	*t*AmylOH	1/500	15	1980
2	**4b**	KO*t*Bu	50	*t*AmylOH	1/500	15	1980
3	**4b**	KO*t*Bu	25	*t*AmylOH	1/500	30	990
4	**4b**[d]	KO*t*Bu	50	*t*AmylOH	1/500	30	990
5	**4b**	KO*t*Bu	50	MeOH	1/500	55	550
6	**4b**	KO*t*Bu	50	EtOH	1/500	30	990
7	**4b**	None	50	*t*AmylOH	1/500	no conversion	–
8	**4a**	KO*t*Bu	50	*t*AmylOH	1/2000	60	1980
9	**4c**	KO*t*Bu	50	*t*AmylOH	1/500	no conversion	–

[a]Precatalyst activated *in situ*: 5 mg (**4a**, **b**, or **c**), 4 equiv $LiAlH_4$ (0.05 mL 1 M in THF), followed by 0.5 mL alcohol; 6 mL THF. [b]Base (C/B = 1/10) dissolved in 4 mL THF and added into the reactor preloaded with THF solution with precatalyst and substrate to commence catalysis. [c]Calculated at 99% conversion. [d]$NaAlH_4$ used instead.

Scheme 3. H_2 hydrogenation of benzaldehyde with an *in situ*-generated catalyst derived from 4b

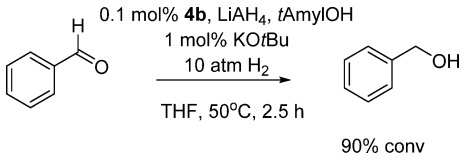

significant improvement in activity over the other iron-based catalysts shown in Figure 1 for the enantioselective hydrogenation of ketones that employ H_2 gas. It is unusual that the (*S*,*S*) chiral catalyst system produces the (*S*) alcohol enantiomer. Typically the (*R*) enantiomer of the alcohol is produced using ligands derived from the (*S*,*S*)-diamine, at least for our iron-based asymmetric transfer hydrogenation catalysts and for most ruthenium diamine-based hydrogenation catalysts.[71−73]

The catalyst mixture starting with **(*S*,*S*)-4d** was tested for acetophenone hydrogenation at both 50 and 25 °C. The enantioselectivity of the reaction increased from 80% to 89% (*S*), while the time for complete conversion lengthened from 30 to 90 min, respectively. The catalytic mixture at 50 °C can accommodate additional loadings of substrate. Four additional batches of acetophenone (1000 equiv) were added in 30-min intervals without slowing down the catalyst, and the ee of the product (*S*)-1-phenylethanol was unaffected. A fifth batch slowed the catalytic reaction, but it still went to completion resulting in a net TON of 5000 (see the Supporting Information, Figure S37). The enantioselectivity of the **(*S*,*S*)-4d** system decreases along with the activity as steric hindrance due to bulky substituents on the ketone substrate increases (Table 2, entry 7 vs 8 vs 9). The low enantioselectivity is not due to racemization, as the reactions were monitored periodically and the ee remained constant until completion. In the case of the less bulky substrate benzylacetone (entry 15), the catalytic reduction by the **(*S*,*S*)-4d** system was rapid, but enantioselectivity was lost (ee = 5%). In the case of the substrate 1-phenyl-2-butanone (entry 16) that is more sterically hindered than benzylacetone, the ee increased to 30%, while there was a substantial decrease in catalytic activity (TOF = 90 h^{-1}). This lower catalytic activity is the result of enolate formation due to the presence of base. Fortunately, the inhibitory effect of enolate, which is likely to be a good ligand for iron, does not poison the catalyst completely. Precatalyst **(*S*,*S*)-4d** was found to give the moderately efficient hydrogenation of nonaromatic ketones (entry 17) but with inferior enantioselectivity (ee =46%). The system was also found to catalyze the reduction of 2-acetylthiophene (entry 18) and 2-acetylfuran (entry 19) to near completion. However, the catalysis was slower (TOF = 240 h^{-1} for 2-acetylthiophene and 220 h^{-1} for 2-acetylfuran) when compared to acetophenone (TOF = 990 h^{-1}). The difference is believed to be due to the stronger binding to the iron of the chelating substrates via the O or S of the heterocycle. However, since catalysis can go to completion, this chelation effect must be reversible. The chelation effect is more pronounced in the case of the substrate 2-acetylpyridine (entry 20) such that catalysis ceased at 20% conversion (or 200 TON) after one hour. It is presumed that the substrate, the alcohol product, or both completely deactivate the catalyst. An increase of the H_2 pressure to 10 atm enabled the hydrogenation of 2-acetylpyridine to 60% conversion (or 600 TON) in two hours and maintained a 74% ee of the hydrogenated product.

Unlike Milstein's iron complexes M2 or M3, the system could not hydrogenate the unsaturated ketone, *trans*-4-phenyl-3-buten-2-one, at 5 or 10 atm H_2 pressure (Table 2, entry 21). The presence of an olefin does not poison the catalyst because the **(*S*,*S*)-4d** system was able to fully hydrogenate 5-hexen-2-one (entry 22) to 5-hexen-2-ol without affecting the olefin as determined by NMR spectroscopy. However, in comparison with benzylacetone (entry 15) where catalytic hydrogenation was complete in one hour, the hydrogenation of 5-hexen-2-one was complete in four hours. Furthermore, upon addition of 1-hexene (500 equiv) to a hydrogenation reaction of acetophenone (1000 equiv), catalysis was complete in 90 min as opposed to 30 min. These results imply there is some degree of reversible olefin coordination analogous to the situation with the heterocyclic substrates (entries 18−20). Enone and diene compounds of iron are known and have been well studied.[74−78] It is postulated that there is some degree of reversible coordination with enones and dienes as well with our iron catalysts because upon addition of *trans*-4-phenyl-3-buten-2-one (500 equiv) to a hydrogenation reaction of acetophenone

dx.doi.org/10.1021/ja4082233 | J. Am. Chem. Soc. XXXX, XXX, XXX−XXX

Table 2. Reactivity of various ketones in the asymmetric hydrogenation reaction using an *in situ*-generated catalyst derived from (*S*,*S*)-4d.[a]

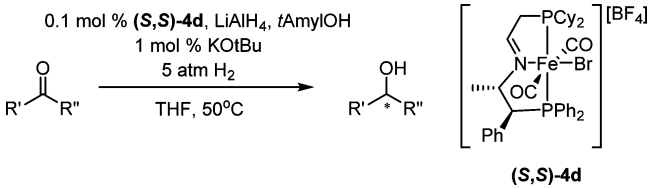

(*S*,*S*)-4d

No.	Substrate	Time (h)	% conv.[b]	e.e.[b] (%)	TOF (h^{-1})	TON
1		0.5	99	80 (*S*)	1980	990
2		1.5	95	80 (*S*)	630	950
3	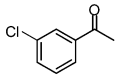	1.3	95	80 (*S*)	730	950
4	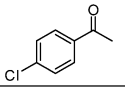	1	99	76 (*S*)	990	990
5	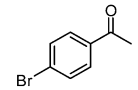	1.5	95	77 (*S*)	630	950
6	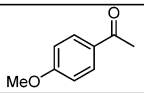	0.8	96	82 (*S*)	1200	960
7	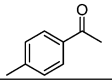	0.6	96	79 (*S*)	1600	960
8	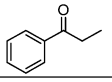	0.8	90	83 (*S*)	1500	900
9	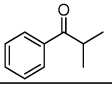	6	90	60 (*S*)	150	900
10	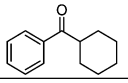	12	80	37 (*S*)	65	800
11	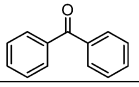	2	95	n/a	500	950
12		18	92	22 (*S*)	50	920
13	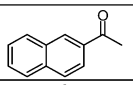	0.5	99	80 (*S*)	1980	990
14		0.8	99	85 (*S*)	1230	990
15	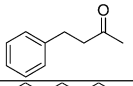	1	97	5 (*S*)	970	970
16	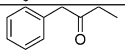	11	97	30 (*S*)	90	970
17		3	91	46 (*S*)	300	910
18	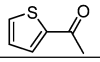	4	95	82 (*S*)	240	950
19	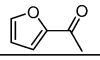	5	90	85 (*S*)	220	900
20	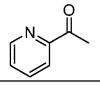	1	20[c]	74 (*S*)[d]	200	200
21	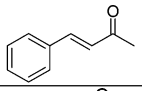	24	0	n/a	0	0
22	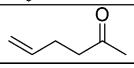	4	95	0	240	950

[a]Catalyst prepared *in situ*: (*S*,*S*)-**4d** (5 mg, 0.007 mmol) mixed with 6 equiv $LiAlH_4$ (0.05 mL of 1 M $LiAlH_4$ in THF) followed by 0.5 mL *t*AmylOH in 6 mL THF. [b]Determined by GC. [c]Determined by ^1H NMR spectroscopy. [d]Determined by HPLC.

(1000 equiv), catalysis was complete in 90 min with zero conversion of the enone additive.

The hydrogenation of imines was also investigated using activated (*S*,*S*)-**4d** under the harsher conditions of 20 atm H_2 gas and at 50 °C at substrate loadings of 1 mol % (based on (*S*,*S*)-**4d**) and 10 mol % base. The system was inactive for the hydrogenation of the imine substrates, *N*-(1-phenylethylidene)-aniline or phenyl-*N*-(1-phenylethylidene)methanamine, or the nitrile substrate, benzylnitrile. However, it did catalyze the complete hydrogenation of the activated imine, *N*-(diphenylphosphonyl)propiophenoneimine in 22 h with a TOF of 5 h^{-1} (Scheme 4). The activity of this system is higher than that of Beller and co-worker's cooperative system B2 which had a TOF of about 1 h^{-1} under harsher conditions.[50] The enantioselectivity of activated (*S*,*S*)-**4d** was high (ee = 90%

Scheme 4. H_2 Hydrogenation of *N*-(Diphenylphosphinoyl)propiophenoneimine Using an *in Situ*-Generated Catalyst Derived from (*S*,*S*)-4d

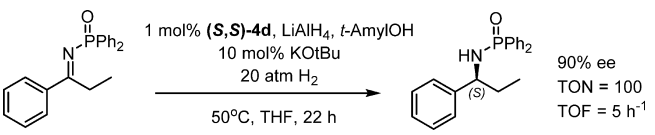

dx.doi.org/10.1021/ja4082233 | J. Am. Chem. Soc. XXXX, XXX, XXX–XXX

Scheme 5. Synthesis and Proposed Structures of Hydride−Aluminum Hydride Iron Complexes 5a−d, 6a−d and the Monohydride Complexes 7b (R‴ Me) and 8b and (*S*,*S*)-8d (R‴ *t*Amyl)

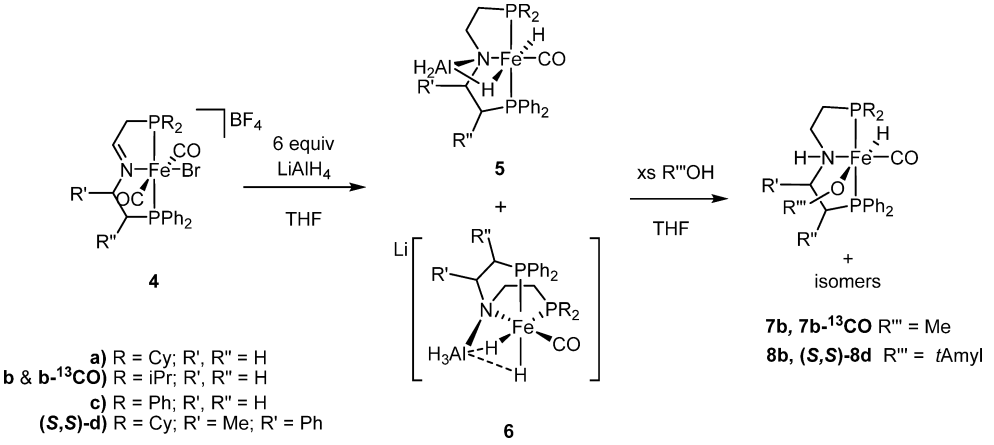

(*S*)), although not as high as the 99% (*R*) obtained for our active transfer hydrogenation iron precatalyst, (*S*,*S*)-[Fe(CO)(Br)($Ph_2PCH_2CHNC(H)PhCH(Ph)NCHCH_2PPh_2$)][$BPh_4$] with TOF = 200 s^{-1}.[34]

Study of the catalyst activation steps. Purple THF solutions of 4a-d turned immediately dark brown and evolved gas upon addition of the $LiAlH_4$ activator (Scheme 5). Removal of the THF solvent and subsequent removal of a black precipitate with Et_2O afforded a dark brown-yellow solution. The isolated residue was examined by NMR spectroscopy and found to contain two iron hydride-aluminum hydride species with either *trans* hydrogens with a *mer*−P−N−P′ ligand on iron (**5a-d**) or *cis* hydrogens with a *fac*−P−N−P′ ligand (**6a-d**) on iron as shown in Scheme 5. For example **5b** is thought to have a *mer* configuration because it has a large J_{PP} of 105 Hz while **6b** is *fac* with a small J_{PP} of 20 Hz. Since no proton source was added to the reaction, we postulate that Al is still bound to the amide as AlH_3. The ^{27}Al NMR spectrum supports this postulate since it displays a large broad signal at 100 ppm. So also does the IR spectrum which has ν_{Al-H} absorptions at 1783 and 1648 cm^{-1}.[79] The compound $H_2Al[N(CH_2CH_2NMe_2)_2]AlH_3$ provides a precedent for such an alane-amide adduct.[80] Unfortunately, many crystallization attempts failed to yield crystals. We rely on extensive NMR spectroscopic and density functional theory analysis to deduce possible structures of the complexes.

There are potentially up to two configurations of structures **5a-d** (H *trans* to H, and H *trans* to N). However only the first is the major one as drawn. For structures **6a-d**, there is only one configuration and its enantiomer for **6a** and **6b** and only one for **6c** (no enantiomer) but there are two diastereomers for (**S**,**S**)-**6d** with the nitrogen in the *R* or *S* configuration. The chemical shifts, coupling constants and analysis including DFT calculations that support the tentative structures of the iron hydride species **5** and **6** shown in Scheme 5 are provided in the SI.

An important observation is that the complexes **5c** and **6c** that form starting with complex **4c** contain symmetrical $PPh_2CH_2CH_2NCH_2CH_2PPh_2$ ligands. This is apparent from the $^{31}P\{^1H\}$ NMR spectrum where **5c** and **6c** give singlets due to the equivalent phosphorus nuclei (see the SI, Figure S14). This is evidence that the imine group is reduced in the starting complexes **4a-d** during catalyst activation.

Since the catalytic hydrogenation activity depended on the nature of the alcohol used in the catalyst activation, the treatment of the iron hydride−aluminum hydride complexes with MeOH and *t*AmylOH were separately examined by NMR. Upon addition of an excess of alcohol to a C_6H_6 or THF solution of complexes **5** and **6**, iron precatalysts *mer*-Fe(H)(OR''')(CO)(P−CH_2NH−P′) (**7** with R‴ = Me; **8** with *t*Amyl) were formed (Scheme 5). The color of the solution changed from yellow to orange along with gas evolution.

The NMR spectra of the isolated residues showed multiple iron hydride complexes with similar patterns; however, they were iron monohydride complexes. The ^{1}H, ^{31}P, and ^{13}C NMR spectra of complexes **7b**, **7b-^{13}CO**, **8b** and (**S**,**S**)-**8d** were examined in detail to distinguish differences between the reaction with MeOH as compared with that with *t*AmylOH. Properties of the major isomers are listed in Table 3. The $^{31}P\{^1H\}$ NMR spectrum demonstrated that there is no dissociation of the P−N−P′ ligands and that there is a downfield shift of the phosphorus resonances for solutions of **8** vs solutions of **7**, thus providing evidence for an alkoxide ligand. The major iron monohydride compounds are postulated to have a *mer*-structure with *trans*-phosphorus groups of the P−N−P′ ligand since the $^2J_{PP}$ are in the range of 120−150 Hz. The $^2J_{HP}$ values of the hydride resonance in the ^{1}H NMR spectrum are greater than 50 Hz, also consistent with structures with hydride *cis* to phosphorus (see the SI). The ^{1}H−^{31}P HMBC NMR spectrum enabled the correlation of the hydride resonances to the appropriate phosphorus resonances for **7b**, **7b-^{13}CO**, and (**S**,**S**)-**8d** (discussed later). The ^{1}H−^{13}C HMBC NMR spectrum of **7b-^{13}CO** showed unique correlations for each hydride to one CO ligand (NMR spectra are provided in SI). Due to the complexity of the 1−4 ppm region of the ^{1}H NMR spectrum with strong solvent and crown ether resonances, 2D experiments to locate the ^{1}H NMR resonance of the hydrogen on nitrogen, for example using ^{15}N−^{1}H HMQC or ^{1}H−^{1}H NOESY, failed.

Therefore, for each isomer there is a *mer*-configuration of the complex with one P−NH−P′, hydride, alkoxide and carbonyl ligand. The *trans* positions for the monodentate ligands are inequivalent because of the position of the NH group. This makes the total number of possible methoxide isomers: six for **7a** and **7b** (and six enantiomers), three for **7c** and six for (**S**,**S**)-**7d**. The *t*Amyl derivatives **8** have the same numbers of isomers.

dx.doi.org/10.1021/ja4082233 | J. Am. Chem. Soc. XXXX, XXX, XXX−XXX

Table 3. NMR Chemical Shifts (THF-d_8) of Iron Precatalysts of Interest

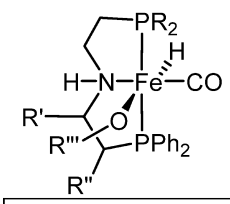	^{1}H NMR (600 MHz) (ppm, ^2J Hz)	^{31}P{^{1}H} NMR (243 MHz) (ppm, ^2J Hz)	^{13}C{^{1}H} NMR (150 MHz) (ppm, ^2J Hz)
7b-^{13}CO isomer I (R''' = Me)	-18.6 (td) J_{HC} = 19 J_{HP} = 52	82.8 (ddd) 102.1 (ddd) J_{PH} = 39[a] J_{PC} = 27 J_{PP} = 119.1	222.3 (td) J_{CH} = 14 J_{CP} = 26
7b-^{13}CO isomer II (R''' = Me)	-21.6 (td) J_{HC} = 20 J_{HP} = 57	77.2 (ddd) 96.7 (ddd) J_{PH} = 41[a] J_{PC} = 27 J_{PP} = 137	224.1 (td) J_{CH} = 17 J_{CP} = 27
7b-CO isomer III (R''' = Me)	-22.7 (dd) J_{HP} = 52, 56	75.0 (dd) 95.7 (dd) J_{PH} = 21[a] J_{PP} = 136	n/a
8b isomer I (R''' = *t*Amyl)	-21.6 (dd) J_{HP} = 52, 56	75.3 (dd) 94.8 (dd) J_{PH} = 30[a] J_{PP} = 137	n/a
8b isomer II (R''' = *t*Amyl)	-26.6 (dd) J_{HP} = 60, 72	64.7 (dd) 86.6 (dd) J_{PH} = 53 J_{PP} = 152	n/a
(*S*,*S*)-8d isomer I (R''' = *t*Amyl)	-21.6 (dd) J_{HP} = 47, 56	95.4 (dd) 86.4 (dd) J_{PH} = 49[a] J_{PP} = 140	n/a
(*S*,*S*)-8d isomer II (R''' = *t*Amyl)	-24.3 (t) J_{HP} = 48	108.5 (d) 98.1 (d) J_{PP} = 148	n/a

[a]Residual coupling due to incomplete decoupling of the high-field hydride resonance.

The two isomers with hydride *trans* to carbonyl are known to be too high in energy (see the DFT results below), whereas the one with hydride *trans* to alkoxide with the alkoxide next to the NH is lowest and is likely to be one of the isomers listed in Table 3. We have not been able to distinguish between the other isomers but see at least three of them.

The relative ratios of the various hydride species **7b** appear to vary slightly, depending on exact reaction conditions; the use of slightly less alcohol favors the formation of the hydride species with ^{1}H NMR signals at −18.6 ppm (Table 3), whereas the use of excess alcohol yields much less of the −18.6 ppm hydride species and a new species with ^{1}H NMR hydride signals at −22.7 ppm. The presence of a separate species which does not correlate to any hydrides is also often detected. This has been assigned as a zero-valent Fe(CO)$_2$(P−CH$_2$NH−P′) complex **9** with ^{31}P{^{1}H} doublets at 101.0 and 79.7 ppm with J_{PP} of 73 Hz. The formation of this complex is associated with the presence of base (see below for its independent synthesis), in this case probably LiOH produced by reaction of the hydrides with traces of water in the solvents. The presence of this complex shows that ligand redistribution reactions are possible. Over a period of 24−48 h the hydride signals at −18.6 ppm and all minor hydride species disappear leaving a spectrum with only two hydride species at −21.6 and −22.7 in a 1:1 ratio. ^{1}H−^{31}P HMBC and ^{1}H−^{13}C HMBC enabled correlation of the hydride to other nuclei for each isomer. The −21.6 ppm hydride is a doublet of doublets with J_{HP} = 52 and 57 Hz, and correlates to ^{31}P doublet of doublets at 94.8 and 75.3 ppm, with J_{PH} = 30 and J_{PP} = 137 Hz. This hydride was also correlated to ^{13}C{^{1}H} NMR signals at 222.8 ppm for CO, 139.7 ppm for *P*−*C*(Ph) and 24.5 ppm for *P*−*C*(*i*Pr). Similarly, the −22.7 ppm hydride is a doublet of doublets with J_{HP} = 52 and 56 Hz, and correlates to ^{31}P doublet of doublets at 95.7 and 75.0 ppm, with J_{PH} = 21 and J_{PP} = 136 Hz, and ^{13}C{^{1}H} NMR signals at 222.4 ppm for CO, 139.5 ppm for *P*−*C*(Ph) and 24.6 ppm for *P*−*C*(*i*Pr). These species are quite similar and are known to be monohydride, monocarbonyl, iron P−N−P species and are therefore proposed to be *mer*-Fe(H)(OMe)(CO)(P−CH$_2$NH−P′), with the N−H up and down, relative to the hydride, for each isomer, respectively. The −21.6 ppm hydride is therefore a kinetic product and the −22.7 ppm hydride, a thermodynamic product.

The labeled alcohol, ^{13}CH$_3$OH, was utilized in the preparation of **7b** in order to attempt to verify the presence of the methoxide ligand. However, only the resonance for free ^{13}CH$_3$OH was detected. This is likely to be due to a dynamic averaging of the methoxide and methanol resonances since alkoxide ligands are usually hydrogen bonded to an alcohol as hydrogen-bonded anions [ROH···OR]$^-$.[81,82] No enhancement of the Fe−^{13}CO signals were detected, and this shows that the isomers of **7b** and any **9** present do not contain carbonyl ligands derived from the alcohol.[83,84]

Preformed solutions of **7b** containing only the two hydride isomers at −21.6 and −22.7 ppm were tested for H$_2$ hydrogenation of acetophenone to 1-phenylethanol under 5 atm H$_2$ pressure and 50 °C, as optimized. These solutions were highly active, converting 1000 equiv of substrate in less than 15 min, but only in the presence of base. The role of the base is under active investigation.

A mixture of hydride complexes **8b** without contamination by complex **9** was also tested for the hydrogenation of acetophenone at 50 °C and H$_2$ pressure of 25 atm in THF in the presence of base (KO*t*Bu). Full conversion of acetophenone to 1-phenylethanol occurred in 10 min with 0.2 mol % catalyst loading based on the initial amount of **4b** used to synthesize **8b**. The synthesis and isolation of the mixture of hydrides **8b** is tedious, and the resulting oily residue is difficult to handle. It is more practical to activate the precatalyst **4b** without the isolation of the hydride intermediates as described above.

The ^{1}H NMR hydride resonances of the alkoxide species **7** and **8** (Table 3) are similar in chemical shift and coupling constant to those of the hydride alkoxide complex Fe{2,6-(P*i*Pr$_2$CH$_2$)$_2$C$_5$H$_3$N}(H)(CO)(OCHPh$_2$) reported by Milstein and co-workers.[39] The latter displays a triplet hydride resonance at −19.9 ppm with J_{HP} = 53 and is thought to be a catalytically active form of precatalyst M2 of Figure 1.

The chiral precatalyst (*S*,*S*)-**8d** also exists as a mixture of iron monohydride compounds with two major isomers (Table 3). Again the large $^2J_{PP}$ indicates *trans* phosphine coordination of the P−CH$_2$N−P′ ligand while the large $^2J_{HP}$ indicates *cis* hydride and phosphine ligands. The chemical shifts of the minor iron monohydride compounds are provided in the SI. However, the phosphorus chemicals shifts of these minor compounds were only identified via the ^{1}H−^{31}P HMBC spectrum and this implies they are in low concentration relative to the two major isomers of (*S*,*S*)-**8d**. Despite the fact that these complexes exist as a mixture of isomers, they are surprisingly active for the hydrogenation of ketones and, in the case of (*S*,*S*)-**8d**, they have surprisingly good enantioselectivity.

dx.doi.org/10.1021/ja4082233 | J. Am. Chem. Soc. XXXX, XXX, XXX−XXX

For example the mixture of hydrides catalyzes the hydrogenation of acetophenone to 1-phenylethanol with same ee and activity as the precatalyst (*S,S*)-**4d** activated *in situ* (Scheme 6).

Scheme 6. Asymmetric Hydrogenation of Acetophenone Catalyzed by the Mixture of Isomers of Alkoxide Hydrides (*S,S*)-8d

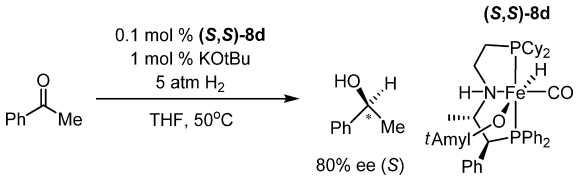

The Properties of Isomeric Alkoxide Hydrides (*S,S*)-7d As Determined by DFT Calculations. In order to support our structural assignments for these alkoxides we investigated the relative stabilities of the possible isomers by DFT studies. The first study utilized a large basis set to treat simplified structures of the methoxide isomers where the phenyls on the phosphorus were replaced with hydrogen, and the cyclohexyl groups and backbone phenyl, with methyl groups. This study was designed to reveal the electronically preferred isomers with the *mer*-P−NH−P′ ligand stereochemistry that has already been established by our NMR studies. Of the six possible diastereomers, the two isomers with hydride *trans* to carbonyl were found to be high in energy and thus too unstable to form (see the SI, Figure S26). The isomer with the hydride *trans* to methoxide and with the methoxide next to the NH group is the most stable. This is the stereochemistry drawn for (*S,S*)-**8d** in Scheme 6.

The effect of sterics on the relative stabilities of the isomers was explored using a gas phase calculation of the full structures treated with a smaller basis set. A summary of the results is shown in Figure 4. There are four diastereomers that are low in energy with the isomer **F** being the most stable. The methoxide oxygen is within hydrogen-bonding distance of the N−H group (O···H 1.75 Å).

Reaction of the Methoxide Hydrides 7b with Base. Base is required for catalysis, but the methoxide hydride complexes **7b** are unstable in the presence of base when the substrate and hydrogen are absent. When KO*t*Bu was added to a C_6H_6 solution of prepared precatalyst **7b** the orange solution turned red after stirring for 10 min. After removal of a white precipitate, the $^{31}P\{^1H\}$ NMR (C_6D_6) spectrum of the isolated red residue showed one major compound as two doublets at 79.7 and 101.0 ppm (J_{PP} = 73 Hz) along with minor compounds and free P−CH_2NH−P′ ligand. Once crystals suitable for X-ray diffraction were isolated by slow diffusion of pentane into the C_6D_6 solution, the major compound was identified to be the neutral Fe(0) complex Fe($Ph_2PCH_2CH_2NHCH_2CH_2PiPr_2$)$(CO)_2$, **9** (Scheme 7, Figure 5).

Complex **9** has a trigonal bipyramidal geometry. The phosphorus atoms of the P−CH_2NH−P′ ligand and a CO ligand are in the equatorial plane, while the second CO ligand and N atom of the P−CH_2NH−P′ ligand occupy the axial positions. The P−Fe−P bond angle is 119.55(2)° and is larger than that observed for the $[Fe(CO)(Br)(P-N-N-P)]^+$ or $[Fe(NCCH_3)_2(P-N-N-P)]^{2+}$ complexes whose P−Fe−P bond angles ranged between 108 and 112°. The existence of the amine in complex **9** provides additional evidence for the

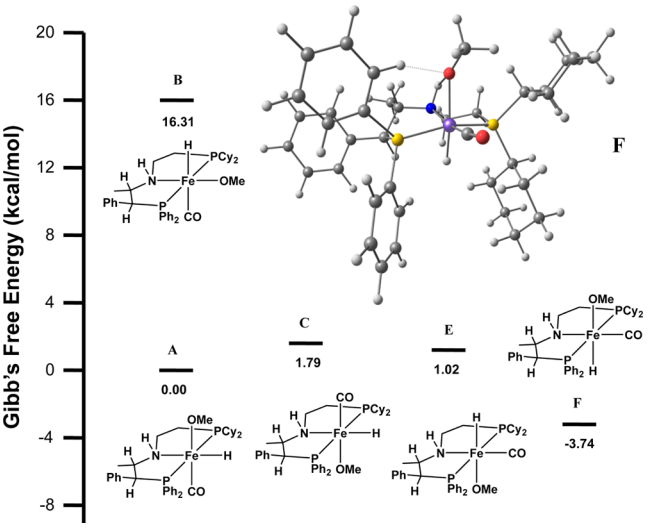

Figure 4. The relative energies of five possible diastereomers of (*S,S*)-**7d**. A sixth high-energy diastereomer, D, with hydride *trans* to CO is not shown. Bond lengths for structure F: Fe−*H* = 1.55, Fe−*C* = 1.69, Fe−*O* = 1.99, Fe-*N* = 2.07, Fe−P (PPh_2) = 2.23, Fe−P (PCy_2) = 2.24 Å, O···HN 1.75 Å. Bond Angles: H−Fe−*C* = 100.9°, H−Fe−P(PCy_2) = 83.7°, H−Fe−P(PPh_2) = 77.8°, H−Fe−*N* = 89.6°, O−Fe−*C* = 95.7°, O−Fe−P(PCy_2) = 92.4°, O−Fe−P(PPh_2) = 102.3°, O−Fe−*N* = 73.7°, Fe−N−*H* = 88.5°, Fe−O−H (N−H) = 75.2°, N−H−*O* = 119.7°, Fe−O−*C* = 126.5°, Fe−C−*O* = 173.7°, C−Fe-*N* = 169.4°, P(PPh_2)−Fe−P(PCy_2) = 158.9°, H−Fe−*O* = 163.2°.

Scheme 7. Synthesis of 9

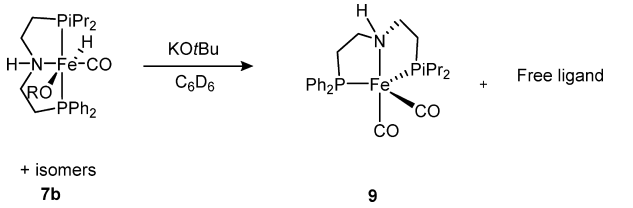

reduction of the P−CH═NH−P′ ligand by $LiAlH_4$. The IR (KBr) spectrum of the isolated residue of **9** showed two intense carbonyl absorptions at 1884 and 1791 cm^{-1}. A similar complex, Fe{2,6-(Ph_2PCH_2)$_2$(C_5H_3N)}$(CO)_2$, was synthesized and characterized by Chirik and co-workers and found to also have a trigonal bipyramidal geometry about the Fe(0) and have a similar IR spectrum.[85] However, the P−N−P ligand of their complex is rigid such that phosphorus atoms are found at the axial positions about the iron center and create a large P−Fe−P bond angle of 165.99(1)°. We were initially surprised that **9** was an Fe(0) compound that had acquired an additional CO ligand, but we found that Milstein and co-workers also observed the formation of the Chirik Fe(0) complex along with free P−N−P ligand and black precipitate when they performed a similar reaction with their well-defined iron hydride precatalyst with base.[39] It is not clear how the reaction to form **9** proceeds. The reaction was conducted under an atmosphere of argon which rules out the possibility of dinitrogen coordination. It is presumed that the second carbonyl ligand is obtained via an intermolecular ligand redistribution reaction still to be characterized. Complex **9** was tested and found to be inactive as a hydrogenation catalyst; hence, we presume this complex forms when H_2 or the substrate is absent.

dx.doi.org/10.1021/ja4082233 | J. Am. Chem. Soc. XXXX, XXX, XXX−XXX

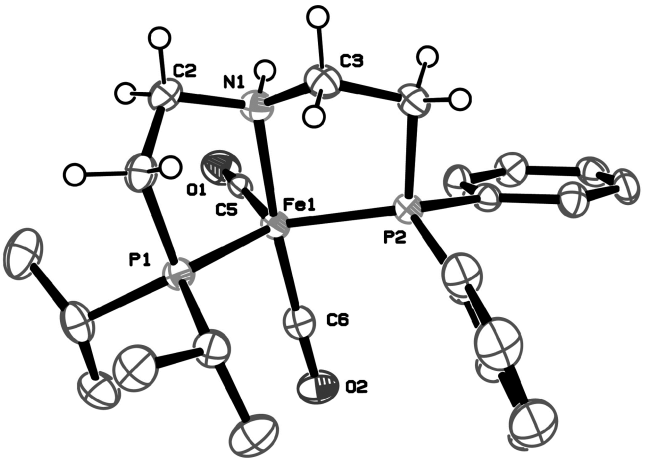

Figure 5. ORTEP plot (thermal ellipsoids at 30% probability) of the X-ray crystal structure of **9**. Hydrogen atoms of phenyl and isopropyl substituents removed for clarity. Selected bond lengths (Å) and angles (deg): Fe(1)−C(6): 1.723(2); Fe(1)−C(5): 1.797(2); Fe(1)−N(1): 2.088(2); Fe(1)−P(2): 2.1735(6); Fe(1)−P(1): 2.2038(6); C(6)−Fe(1)−C(5): 93.94(9); C(6)−Fe(1)−N(1): 172.41(9); C(5)−Fe(1)−N(1): 93.07(8); C(6)−Fe(1)−P(2): 89.62(7); C(5)−Fe(1)−P(2): 120.34(6); C(5)−Fe(1)−P(1): 119.37(6); P(2)−Fe(1)−P(1): 119.55(2); N(1)−Fe(1)−P(2): 84.34(5); C(6)−Fe(1)−P(1): 95.00(7).

■ CONCLUSIONS

We have developed an effective synthesis templated by iron(II) to make unsymmetrical P−N−P′ ligands by the condensation of phosphine-amines with phosphine-aldehydes, generated from phosphonium dimers. A mixture of *trans*- and *cis*-iron complexes, $Fe(CO)(Br)_2(P{-}CH{=}N{-}P')$, **2** and **3**, were initially synthesized from the one-pot reaction with phosphonium dimers (**1a**−**c**), KO*t*Bu, $FeBr_2$ and $PhP_2C_2H_4NH_2$ in THF under a CO(g) atmosphere. Upon addition of $AgBF_4$ to these complexes under a CO atmosphere, the new complexes *trans*-$[Fe(CO)_2(Br)(P{-}CHN{-}P')][BF_4]$ (**4a**−**d**) were synthesized in high yield. Complexes **4a**−**d** were reacted with $LiAlH_4$, followed by alcohol, to generate a mixture of iron hydride complexes with the proposed structures *mer*-$Fe(H)(CO)(OR)(P{-}CH_2NH{-}P')$ (where R = Me or *t*Amyl). The mixture of monohydride iron precatalysts **7a**, **7b**, or (***S,S*)-8d** that have alkyl substituents on one of the phosphorus atoms of the P−CH_2NH−P′ ligand are active for the H_2 hydrogenation of ketones and aldehydes under mild basic conditions (T = 50 °C, $p(H_2)$ = 5 atm). Catalytic performance reached TOF up to 2000 h^{-1}, TON up to 5000, and enantioselectivities up to 85% (*S*). It has not been established yet how many of the diastereomeric hydrides lead to active catalysts. Nevertheless, we have shown that a variety of such iron hydride compounds can be prepared in a few steps from aldehyde and amine building blocks on Fe(II). A more well-defined hydride system will be needed to study the mechanism of catalysis in more detail and further improve the catalyst performance.

■ EXPERIMENTAL SECTION

General Comments. All procedures and manipulations involving air-sensitive materials were performed under an argon or nitrogen atmosphere using Schlenk techniques or a glovebox with N_2(g). Solvents were degassed and dried using standard procedures prior to all manipulations and reactions. Deuterated solvents were purchased from Cambridge Isotope Laboratories or Sigma-Aldrich, degassed, and dried over activated molecular sieves prior to use. All liquid ketone substrates were vacuum distilled, degassed, and stored over activated molecular sieves. Phosphonium dimers, **1a**−**c**,[52,86] and $Fe(CO)_4(Br)_2$[87] were synthesized according to literature procedures. 2-(Diphenylphosphino)ethylamine was donated by Digital Specialty Chemicals. All other reagents were purchased from Sigma-Aldrich or Strem Chemicals and utilized without further purifications. NMR spectra were recorded at ambient temperature and pressure using Varian VnmrS-400 and Agilent DD2-600 [^{1}H (400, 600 MHz), ^{13}C{^{1}H} (100, 150 MHz), ^{31}P{^{1}H} (161, 242 MHz), ^{19}F{^{1}H} (356 MHz)]. The ^{31}P chemical shifts were measured relative to 85% H_3PO_4 as an external reference. The ^{19}F chemical shifts were referenced relative to $CFCl_3$. In the synthesis of **2a** and **2b**, photolysis was performed using a 450 W mercury vapor lamp (model: Hanovia UV medium pressure 450 W immersion lamp). The elemental analyses were performed on a Perkin-Elmer 2400 CHN elemental analyzer. Some complexes gave unsatisfactory carbon analyses but acceptable hydrogen and nitrogen content because of a combustion problem due to the tetrafluoroborate anion.[88]

***trans*-Fe(Ph$_2$PCH$_2$CH$_2$NCHCH$_2$PCy$_2$)(CO)(Br)$_2$, 2a.** A vial was charged with **1a** (80 mg, 0.125 mmol) and KO*t*Bu (28 mg, 0.249 mmol) and 25 mL benzene. The slurry was allowed to stir for 10 min by which time the mixture turned cloudy and then was filtered into a Schlenk flask. To this solution was added 2-(diphenylphosphino)ethylamine (57 mg, 0.249 mmol) followed by $Fe(CO)_4(Br)_2$ (81 mg, 0.249 mmol). The mixture immediately evolved gas in addition to turning orange in color. The flask was immediately exposed to UV light and was allowed to stir for 6 h or until the solution turned red-purple. The flask was removed from the UV source and filtered through a pad Celite to remove all precipitates. The solvent was concentrated, and pentane (10 mL) was added to cause precipitation of a pale-pink solid. The solid was washed with pentane (5 mL) and dried under vacuum. Yield: 35% (60 mg). ^{1}H NMR (400 MHz, C_6D_6) δ: 1.18−1.95 (m, *H*Cy), 2.47 (m, 2H, C*H*$_2$PCy$_2$), 2.66 (m, 2H, C*H*Cy), 2.79 (m, 2H, C*H*$_2$PPh$_2$), 4.11 (m, 2H, C*H*$_2$N), 6.94 (m, 2H, *H*Ph), 7.05 (m, 4H, *H*Ph), 7.91 (m, 5H, *H*Ph, C*H*N). ^{13}C {^{1}H} NMR (100 MHz, C_6D_6) δ: 26.5 (*C*Cy), 27.9 (*C*Cy), 28.7 (*C*H$_2$PPh$_2$), 29.9 (*C*Cy), 30.6 (*C*H$_2$PCy$_2$), 36.4 (*C*Cy), 62.6 (*C*H$_2$N), 129.5 (*C*Ph), 133.1 (*C*Ph), 135.7 (*C*Ph), 146.6 (*C*Ph), 173.3 (*C*HN), 227.8 (br t, J_{PC} = 24.0 Hz, CO). ^{31}P {^{1}H} NMR (161 MHz, C_6D_6) δ: 68.2 (d, J_{PP} = 174 Hz), 71.2 (d, J_{PP} = 174 Hz) ppm. IR (KBr) 1945 cm^{-1} ($\nu_{C\equiv O}$). Anal. Calcd for $C_{29}H_{39}NOP_2FeBr_2$: C, 50.10; H, 5.65; N, 2.01; Found: C, 49.52; H, 5.88; N, 1.75. MS (ESI, methanol/water; m/z^+): 586.1 $[C_{28}H_{39}NP_2FeBr]^+$.

***trans*-Fe(Ph$_2$PCH$_2$CH$_2$NCHCH$_2$PiPr$_2$)(CO)(Br)$_2$, 2b.** The pale-pink solid product was synthesized and isolated using the procedure outlined for 2a: **1b** (80 mg, 0.166 mmol); KO*t*Bu (38 mg, 0.331 mmol); 2-(diphenylphosphino)ethylamine (76 mg, 0.331 mmol); $Fe(CO)_4(Br)_2$ (108 mg, 0.331 mmol). Yield: 25% (50 mg). ^{1}H NMR (400 MHz, C_6D_6) δ: 0.90 (dd, J_{HP} = 7, 14 Hz, 1H, C*H*(CH$_3$)$_2$), 1.21 (dd, J_{HP} = 7, 13 Hz, 6H, C*H*$_3$), 1.44 (dd, J_{HP} = 7, 13 Hz, 6H, C*H*$_3$), 1.70 (dd, J_{HP} = 7, 16 Hz, 1H, C*H*(CH$_3$)$_2$), 2.74 (m, 2H, C*H*$_2$PiPr$_2$) 2.77 (m, 2H, C*H*$_2$PPh$_2$), 4.13 (m, J_{HP} = 20.6 Hz, 2H, C*H*$_2$N), 6.93 (m, 4H, *H*Ph), 7.04 (m, 2H, *H*Ph), 7.22 (indirectly determined from ^{1}H−^{13}C HSQC, C*H*N), 7.89 (m, 2H, *H*Ph), 7.98 (m, 2H, *H*Ph), 8.45 (m, 1H, *H*Ph). ^{13}C {^{1}H} NMR (100 MHz, C_6D_6) δ: 19.35 (*C*H$_3$), 19.5 (*C*H(CH$_3$)$_2$), 20.5 (*C*H$_3$), 25.8 (CH(*C*H$_3$)$_2$), 28.2 (d, J_{CP} = 20 Hz, *C*H$_2$PPh$_2$), 38.0 (d, J_{CP} =

dx.doi.org/10.1021/ja4082233 | J. Am. Chem. Soc. XXXX, XXX, XXX−XXX

17 Hz, CH_2PiPr_2), 61.3 (CH_2N), 129.4 (*C*Ph), 131.5 (*C*Ph), 132.8 (*C*Ph), 135.3 (*C*Ph), 171.8 (*C*HN), 227.9 (t, J_{CP} = 23.8 Hz, *C*O). ^{31}P {^1H} NMR (161 MHz, C_6D_6) δ: 67.4 (d, J_{PP} = 176 Hz), 79.7 (d, J_{PP} = 176 Hz) ppm. IR (KBr) 1945 cm^{-1} ($\nu_{C\equiv O}$). Anal. Calcd for $C_{23}H_{31}NOP_2FeBr_2$: C, 44.91; H, 5.08; N, 2.28; Found: C, 43.99; H, 5.12; N, 2.30. MS (ESI, methanol/water; m/z^+): 507.2 $[C_{22}H_{31}NP_2FeBr]^+$.

***trans*-[Fe(Ph$_2$PCH$_2$CH$_2$NCHCH$_2$PCy$_2$)(CO)$_2$(Br)][BF$_4$], 4a.** A Schlenk flask was charged with **1a** (200 mg, 0.311 mmol) and KO*t*Bu (70 mg, 0.623 mmol) and 25 mL THF. The slurry was allowed to stir for 10 min by which time the mixture turned cloudy. To this solution 2-(diphenylphosphino)ethylamine (143 mg, 0.623 mmol) followed by $FeBr_2$ (204 mg, 0.934 mmol). The Schlenk flask was then exposed to an atmosphere of CO (~2 atm); upon exposure to CO, the pale yellow slurry immediately turned dark purple. The reaction was allowed to stir for 5 h by which time the reaction mixture was red-purple in color. The solvent was removed and the residue was taken up in 25 mL dichloromethane. The solution was filtered through a pad of Celite into a new Schlenk flask and exposed again to a CO atm. $AgBF_4$ (130 mg, 0.668 mmol) in 5 mL THF was injected into the reaction mixture. The solution immediately changed to a bright purple color. After stirring for 30 min, the solvent was removed, taken up in dichloromethane and filtered through a pad of Celite to remove a gray precipitate. The solvent was concentrated and pentane (10 mL) was added to cause precipitation of a purple solid. The solid was washed with pentane (5 mL) and dried under vacuum. Yield: 89% (400 mg). ^1H NMR (400 MHz, CD_2Cl_2) δ: 1.16–2.50 (m, 22H, *H*Cy), 2.50 (m, 2H, CH_2PCy_2), 2.92 (m, 2H, CH_2PPh_2), 3.63 (m, 2H, CH_2N), 7.56–7.95 (m, 11H, *H*Ph, *H*CN). ^{13}C {^1H} NMR (100 MHz, CD_2Cl_2) δ: 25.7 (*C*Cy), 27.2 (*C*Cy), 28.5 (*C*Cy), 28.8 (*C*Cy), 37.5 (CH_2PPh_2), 37.7 (CH_2PCy_2), 63.6 (CH_2N), 129.4 (*C*Ph), 131.0 (*C*Ph), 131.8 (*C*Ph), 182.0 (HCN), 211.5 (dd, J_{CP} = 22, 25 Hz, *C*O). ^{31}P {^1H} NMR (161 MHz, CD_2Cl_2) δ: 45.7 (d, J_{PP} = 85 Hz, *P*Ph$_2$), 70.8 (d, J_{PP} = 85 Hz, *P*Cy$_2$). $^{19}F\{^1H\}$ NMR (356 MHz, CD_2Cl_2) δ: −155.5 (s, BF_4) ppm. IR (KBr) 2005 cm^{-1} ($\nu_{C\equiv O}$). Anal. Calcd for $C_{30}H_{39}NO_2P_2FeBrBF_4$: C, 49.35; H, 5.38; N, 1.92; Found: C, 45.94; H, 5.47; N, 1.52. MS (ESI, methanol/water; m/z^+): 644.1 $[C_{30}H_{39}NO_2P_2FeBr]^+$.

***trans*-[Fe(Ph$_2$PCH$_2$CH$_2$NCHCH$_2$PiPr$_2$)(CO)$_2$(Br)][BF$_4$], 4b.** The purple solid product was synthesized and isolated using the procedure outlined for **4a**: **1b** (200 mg, 0.415 mmol); KO*t*Bu (93 mg, 0.830 mmol); 2-(diphenylphosphino)ethylamine (190 mg, 0.830 mmol); $FeBr_2$ (271 mg, 1.245 mmol); $AgBF_4$ (201 mg, 1.035 mmol). Yield: 83% (450 mg). ^1H NMR (400 MHz, CD_2Cl_2) δ: 1.13 (m, 2H, $CH(CH_3)_2$), 1.45 (m, 12H, CH_3), 2.78 (m, 2H, CH_2PiPr_2), 2.90 (m, 2H, CH_2PPh_2), 3.62 (m, 2H, CH_2N), 7.53 (m, 4H, *H*Ph), 7.91 (m, 7H, *H*Ph, *CH*N). ^{13}C {^1H} NMR (100 MHz, CD_2Cl_2) δ: 15.5 ($CH(CH_3)_2$), 19.1 (CH_3), 28.2 (CH_2PiPr_2), 28.3 (CH_2PPh_2), 63.0 (CH_2N), 129.8 (*C*Ph), 131.8 (*C*Ph), 132.1 (*C*Ph), 181.7 (HCN), 211.5 (dd, J_{CP} = 22, 25 Hz, CO). ^{31}P {^1H} NMR (161 MHz, CD_2Cl_2) δ: 45.5 (d, J_{PP} = 86 Hz, *P*Ph$_2$), 78.2 (d, J_{PP} = 86 Hz, *P*iPr$_2$). $^{19}F\{^1H\}$ NMR (356 MHz, CD_2Cl_2) δ: −155.5 (s, BF_4) ppm. IR (KBr) 2011 cm^{-1} ($\nu_{C\equiv O}$). Anal. Calcd for $C_{24}H_{31}NO_2P_2FeBr_2BF_4$: C, 44.35; H, 4.81; N, 2.15; Found: C, 43.21; H, 4.88; N, 2.09. MS (ESI, methanol/water; m/z^+): 563.2 $[C_{24}H_{31}NP_2O_2FeBr]^+$.

***trans*-[Fe(Ph$_2$PCH$_2$CH$_2$NCHCH$_2$PPh$_2$)(CO)$_2$(Br)][BF$_4$], 4c.** The purple solid product was synthesized and isolated using the procedure outlined for **4a**: **1c** (200 mg, 0.324 mmol); KO*t*Bu (73 mg, 0.648 mmol); 2-(diphenylphosphino)ethylamine (149 mg, 0.648 mmol); $FeBr_2$ (208 mg, 0.971 mmol); $AgBF_4$ (157 mg, 0.809 mmol). Yield: 50% (230 mg). ^1H NMR (400 MHz, CD_2Cl_2) δ: 2.16 (m, 2H, CH_2PPh_2), 2.99 (m, 2H, CH_2N), 3.77 (m, 2H, CH_2PPh_2), 7.54–7.94 (m, 21H, *H*Ph, *CH*N). ^{13}C {^1H} NMR (100 MHz, CD_2Cl_2) δ: 29.2 (CH_2PPh_2), 31.7 (CH_2Ph_2), 62.5 (CH_2N), 129.4 (*C*Ph), 131-.6–132.2 (*C*Ph), 182.4 (*C*HN), 208.8 (br t, J_{CP} = 24 Hz, *C*O). ^{31}P {^1H} NMR (161 MHz, CD_2Cl_2) δ: 47.4 (d, J_{PP} = 95 Hz, *P*Ph$_2$), 51.9 (d, J_{PP} = 95 Hz, *P*Cy$_2$). $^{19}F\{^1H\}$ NMR (356 MHz, CD_2Cl_2) δ: −155.5 (s, BF_4) ppm. IR (KBr) 2016 cm^{-1} ($\nu_{C\equiv O}$). Anal. Calcd for $C_{30}H_{27}NO_2P_2FeBrBF_4$: C 50.18; H, 3.79; N, 1.92; Found: C, 44.38; H, 4.21; N, 1.58. MS (ESI, methanol/water; m/z^+): 632.0 $[C_{30}H_{27}NO_2P_2FeBr]^+$.

***trans*-(*S*,*S*)-[Fe(Ph$_2$PCH(Ph)CH(Me)NCHCH$_2$PCy$_2$)-(CO)$_2$(Br)][BF$_4$], (*S*,*S*)-4d.** The red-purple solid product was synthesized and isolated using the procedure outlined for **4a**: **1a** (100 mg, 0.156 mmol); KO*t*Bu (35 mg, 0.312 mmol); (*S*,*S*)-$Ph_2PCH(Ph)CH(Me)NH_2$ (100 mg, 0.312 mmol); $FeBr_2$ (100 mg, 0.312 mmol); $AgBF_4$ (70 mg, 0.359 mmol). Yield: 82% (200 mg). ^1H NMR (400 MHz, THF-d_8) δ: 0.72–2.05 (m, *H*Cy), 1.11 (CH_3, indirectly determined via $^1H-^1H$ COSY), 2.21 (m, 1H, *H*Cy), 2.61 (m, 1H, *H*Cy), 3.43 (CH_2PCy_2, indirectly determined via $^1H-^1H$ COSY), 3.67 (CH_2PCy_2, indirectly determined via $^1H-^1H$ COSY), 3.85 (m, 1H, *C*H(Me)), 4.14 (m, 1H, *C*H(Ph)), 6.80–7.97 (m, 16H, *H*Ph), 7.96 (d, indirectly determined via $^1H-^1H$ COSY, J_{HP} = 20 Hz, *CH*N). ^{13}C {^1H} NMR (100 MHz, THF-d_8) δ: 12.5 (*C*Cy), 17.2 (*C*Cy), 21.3 (*C*Cy), 27.1 (*C*Cy), 28.4 (*C*Cy), 35.4 (CH_2PCy_2), 37.3 (*C*Cy), 38.2 (*C*Cy), 51.8 (*C*H(Ph)), 70.4 (*C*H(Me)), 126.0–135.3 (*C*Ph), 179.3 (*C*HN), 210.5 (br t, J_{CP} = 23.5 Hz, *C*O), 214.7 (br t, J_{CP} = 21.3 Hz, *C*O). ^{31}P {^1H} NMR (161 MHz, THF-d_8) δ: 69.2 (d, J_{PP} = 81 Hz), 67.8 (d, J_{PP} = 81 Hz). $^{19}F\{^1H\}$ NMR (356 MHz, THF-d_8) δ: −155.9 (s, BF_4) ppm. IR (KBr) 2000.0 cm^{-1} ($\nu_{C\equiv O}$). Anal. Calcd for $C_{37}H_{45}NO_2P_2FeBrBF_4$: C 54.17; H, 5.53; N, 1.71; Found: C, 46.31; H, 6.08; N, 1.05. MS (ESI, methanol/water; m/z^+): 734.1 $[C_{37}H_{45}NO_2P_2FeBr]^+$.

General Procedure for the Synthesis of Complexes 5a–d and 6a–d. A vial was charged with $[Fe(CO)_2(Br)(P-CH{=}N-P')][BF_4]$ (~20 mg) in THF (5 mL) to yield a bright purple solution to which $LiAlH_4$ was added until the solution turned dark yellow-brown (~20 mg). After stirring for 10 min, the solvent was removed and the residue was taken up with ether (5–10 mL) to remove the gray-black precipitate. 12-crown-4 (~4–5 drops) was added to cause the precipitation of an off-white solid ($[Li(12\text{-crown-}4)]BH_4$). The resulting solution was filtered and dried *in vacuo* to yield a yellow residue.

General Procedure for the Synthesis of Complexes 7 and 8. Following the same procedure as outlined for the synthesis of **5a–d and 6a–d**, an excess of alcohol (MeOH or *t*AmylOH) was added dropwise to the final Et_2O solution until gas evolution ceased (~10 drops). The yellow solution turned orange. The solvent was removed, and the residue was taken up with pentane and filtered. The solution was dried *in vacuo* to afford an orange residue.

General Procedure for Hydrogenation Studies. All of the hydrogenation reactions were performed at constant pressures using a stainless steel 50 mL Parr hydrogenation reactor. The temperature was maintained at 50 °C using a constant temperature water bath. The reactor was flushed several times with hydrogen gas at 5 atm prior to the addition of catalyst and substrate, and base solutions. For standard

dx.doi.org/10.1021/ja4082233 | J. Am. Chem. Soc. XXXX, XXX, XXX–XXX

catalysis with *in situ* prepared catalysts, a vial was charged with $[Fe(CO)_2(Br)(P{-}CH{=}N{-}P')]BF_4$ (5 mg, 0.006 mmol) and 3 mL THF. To this solution, 0.05 mL of $LiAlH_4$ (1 M in THF) was added, and the color of the solution immediately changed from purple to a golden brown. After stirring for 5 min, 2-methyl-2-butanol (0.5 mL) was added; the solution was allowed to stir for 10 min or until gas evolution ceased. The solution was transferred to a syringe equipped with a 12 in. needle. The same vial was then charged with substrate (6.095 mmol) and 3 mL THF. The solution was taken up into the same syringe that already contained the precatalyst solution; the needle was then stoppered. For catalysis with preformed species **7b** and **(*S*,*S*)-8d**, NMR solutions (THF-d_8) were transferred to a vial in a nitrogen-filled glovebox, and THF (6 mL) and substrate (6.095 mmol) were added. The solution was transferred to a syringe equipped with a 12 in. needle and stoppered. A second vial was charged with KO*t*Bu (10 mg, 0.089 mmol) and 3 mL THF. This solution was transferred to a second syringe equipped with a 12 in. needle and stoppered as well. Both syringes were taken out of the glovebox and injected to the prepared Parr reactor against a flow of hydrogen gas. Small aliquots of the reaction mixture were quickly withdrawn with a syringe and needle under a flow of hydrogen at timed intervals. Alternatively, small aliquots of the reaction mixture were sampled from a stainless-steel sampling dip tube attached to a modified Parr reactor. The dip tube was 30 cm in length with an inner diameter of 0.01 in., and a swing valve was attached to the end of the sampling tube. All samples for gas chromatography (GC) analyses were diluted to a total volume of approximately 1 mL using oxygenated ethanol. All conversions were reported as an average of two runs. The reported conversions were reproducible. The conversion and enantiomeric excess of hydrogenated ketones were analyzed by a Perkin-Elmer Clarus 400 chromatograph equipped with a chiral column (CP chirasil-Dex CB 25 m × 2.5 mm) with an autosampling capability used for GC analyses. Hydrogen was used as a mobile phase at a column pressure of 5 psi with a split flow rate of 50 mL/min. The injector temperature was 250 °C, and the FID temperature was 275 °C. The oven temperatures and the retention times (t_{SM}, t_R, t_S /min) for substrates are provided in the SI.

Computation. Density functional theory calculations on the models of **5** and **6**, and simplified models of **(*S*,*S*)-7d** were performed using Gaussian 09.[89] The M06 hybrid functional was used for all calculations.[90,91] All atoms were treated with the 6-31++G(d,p) basis set. A pruned (99,590) integration grid was used throughout (Grid = UltraFine). Optimizations were performed in tetrahydrofuran using the integral equation formalism polarizable continuum model (IEF-PCM) with radii and non-electrostatic terms from the SMD solvation model.[92] Full vibrational and thermochemical analyses (1 atm, 298 K) were performed on optimized structures to obtain solvent-corrected free energies ($G°$) and enthalpies ($H°$). Optimized ground states were found to have zero imaginary frequencies. DFT gas phase calculations on the full structures of the isomers of **(*S*,*S*)-7d** were performed using GAMESS.[93,94] The M06 functional was used. Iron was treated with the LANL2DZ basis set with an effective core potential.[95] Atoms C, H, N, O, and P were treated with the 6-31G basis set.

■ ASSOCIATED CONTENT

Ⓢ Supporting Information

Detailed information regarding limitations of the UV template reaction, analysis of the NMR spectra of the iron hydride-aluminum hydride compounds **5a−c** and **6a−c**, and alkoxide complexes **7b**, **7b−^{13}CO**, **(*S*,*S*)-8d**, DFT calculation details, the complete reference 89, energies, structures and coordinates and CIF file of all crystallographic data. This material is available free of charge via the Internet at http://pubs.acs.org.

■ AUTHOR INFORMATION

Corresponding Author

rmorris@chem.utoronto.ca

Notes

The authors declare no competing financial interest.

■ ACKNOWLEDGMENTS

NSERC is thanked for a Discovery Grant to R.H.M., and OGS and OGSST are thanked for scholarships to P.O.L. Digital Specialty Chemicals donated the 2-(diphenylphosphino)ethylamine. Demyan E. Prokopchuk is thanked for preliminary DFT calculations of iron dihydride compounds. Dmitry Pichugin is thanked for aiding with NMR spectroscopy. Computations were performed on the General Purpose Cluster supercomputer at the SciNet HPC Consortium. SciNet is funded by the Canada Foundation for Innovation under the auspices of Compute Canada, the Government of Ontario, Ontario Research Fund - Research Excellence, and the University of Toronto.

■ REFERENCES

(1) *Catalysis without Precious Metals*; Bullock, R. M., Ed.; Wiley-VCH: Hoboken, NJ, 2010.
(2) Tondreau, A. M.; Darmon, J. M.; Wile, B. M.; Floyd, S. K.; Lobkovsky, E.; Chirik, P. J. *Organometallics* **2009**, *28*, 3928−3940.
(3) Monfette, S.; Turner, Z. R.; Semproni, S. P.; Chirik, P. J. *J. Am. Chem. Soc.* **2012**, *134*, 4561−4564.
(4) Sylvester, K. T.; Chirik, P. J. *J. Am. Chem. Soc.* **2009**, *131*, 8772−8774.
(5) Wu, J. Y.; Stanzl, B. N.; Ritter, T. *J. Am. Chem. Soc.* **2010**, *132*, 13214−13216.
(6) Dong, Z. R.; Li, Y. Y.; Yu, S. L.; Sun, G. S.; Gao, J. X. *Chin. Chem. Lett.* **2012**, *23*, 533−536.
(7) Vasudevan, K. V.; Scott, B. L.; Hanson, S. K. *Eur. J. Inorg. Chem.* **2012**, 4898−4906.
(8) Zhang, G.; Scott, B. L.; Hanson, S. K. *Angew. Chem., Int. Ed.* **2012**, *51*, 12102−12106.
(9) Harman, W. H.; Peters, J. C. *J. Am. Chem. Soc.* **2012**, *134*, 5080−5082.
(10) Federsel, C.; Ziebart, C.; Jackstell, R.; Baumann, W.; Beller, M. *Chem.—Eur. J.* **2012**, *18*, 72−75.
(11) Werkmeister, S.; Fleischer, S.; Junge, K.; Beller, M. *Chem.—Asian J.* **2012**, *7*, 2562−2568.
(12) Huisman, G. W.; Liang, J.; Krebber, A. *Curr. Opin. Chem. Biol.* **2010**, *14*, 122−129.
(13) Savile, C. K.; Janey, J. M.; Mundorff, E. C.; Moore, J. C.; Tam, S.; Jarvis, W. R.; Colbeck, J. C.; Krebber, A.; Fleitz, F. J.; Brands, J.; Devine, P. N.; Huisman, G. W.; Hughes, G. J. *Science* **2010**, *329*, 305−309.
(14) Ringenberg, M. R.; Ward, T. R. *Chem. Commun.* **2011**, *47*, 8470−8476.
(15) Matsuda, T.; Yamanaka, R.; Nakamura, K. *Tetrahedron: Asymmetry* **2009**, *20*, 513−557.

(16) Stephan, D. W.; Greenberg, S.; Graham, T. W.; Chase, P.; Hastie, J. J.; Geier, S. J.; Farrell, J. M.; Brown, C. C.; Heiden, Z. M.; Welch, G. C.; Ullrich, M. *Inorg. Chem.* **2012**, *50*, 12338−12348.
(17) Rueping, M.; Dufour, J.; Schoepke, F. R. *Green Chem.* **2011**, *13*, 1084−1105.
(18) Sumerin, V.; Chernichenko, K.; Nieger, M.; Leskelä, M.; Rieger, B.; Repo, T. *Adv. Synth. Catal.* **2011**, *353*, 2093−2110.
(19) Farrell, J. M.; Hatnean, J. A.; Stephan, D. W. *J. Am. Chem. Soc.* **2012**, *134*, 15728−15731.
(20) Farrell, J. M.; Heiden, Z. M.; Stephan, D. W. *Organometallics* **2011**, *30*, 4497−4500.
(21) Mahdi, T.; Heiden, Z. M.; Grimme, S.; Stephan, D. W. *J. Am. Chem. Soc.* **2012**, *134*, 4088−4091.
(22) Reddy, J. S.; Xu, B.-H.; Mahdi, T.; Fröhlich, R.; Kehr, G.; Stephan, D. W.; Erker, G. *Organometallics* **2012**, *31*, 5638−5649.
(23) Morris, R. H. *Chem. Soc. Rev.* **2009**, *38*, 2282−2291.
(24) Junge, K.; Schroder, K.; Beller, M. *Chem. Commun.* **2011**, *47*, 4849−4859.
(25) Darwish, M.; Wills, M. *Catal. Sci. Technol.* **2012**, *2*, 243−255.
(26) Gopalaiah, K. *Chem. Rev.* **2013**, *113*, 3248−3296.
(27) Le Bailly, B. A. F.; Thomas, S. P. *RSC Adv.* **2012**, *1*, 1435−1445.
(28) Sui-Seng, C.; Freutel, F.; Lough, A. J.; Morris, R. H. *Angew. Chem., Int. Ed.* **2008**, *47*, 940−943.
(29) Zhou, S.; Fleischer, S.; Junge, K.; Das, S.; Addis, D.; Beller, M. *Angew. Chem., Int. Ed.* **2010**, *49*, 8121−8125.
(30) Mikhailine, A.; Lough, A. J.; Morris, R. H. *J. Am. Chem. Soc.* **2009**, *131*, 1394−1395.
(31) Mikhailine, A. A.; Morris, R. H. *Inorg. Chem.* **2010**, *49*, 11039−11044.
(32) Lagaditis, P. O.; Lough, A. J.; Morris, R. H. *Inorg. Chem.* **2010**, *49*, 10057−10066.
(33) Sues, P. E.; Lough, A. J.; Morris, R. H. *Organometallics* **2011**, *30*, 4418−4431.
(34) Lagaditis, P. O.; Lough, A. J.; Morris, R. H. *J. Am. Chem. Soc.* **2011**, *133*, 9662−9665.
(35) Mikhailine, A. A.; Maishan, M. I.; Lough, A. J.; Morris, R. H. *J. Am. Chem. Soc.* **2012**, *134*, 12266−12280.
(36) Prokopchuk, D. E.; Morris, R. H. *Organometallics* **2012**, *31*, 7375−7385.
(37) Zuo, W.; Li, Y.; Lough, A. J.; Morris, R. H. *Science* **2013**, *342*, 1080−1083.
(38) Mikhailine, A. A.; Maishan, M. I.; Morris, R. H. *Org. Lett.* **2012**, *14*, 4638−4641.
(39) Langer, R.; Leitus, G.; Ben-David, Y.; Milstein, D. *Angew. Chem., Int. Ed.* **2011**, *50*, 2120−2124.
(40) Langer, R.; Iron, M. A.; Konstantinovski, L.; Diskin-Posner, Y.; Leitus, G.; Ben-David, Y.; Milstein, D. *Chem.—Eur. J.* **2012**, *18*, 7196−7209.
(41) Yang, X. *Inorg. Chem.* **2011**, *50*, 12836−12843.
(42) Gunanathan, C.; Ben-David, Y.; Milstein, D. *Science* **2007**, *317*, 790−792.
(43) Gunanathan, C.; Milstein, D. *Acc. Chem. Res.* **2011**, *44*, 588−602.
(44) Bichler, B.; Holzhacker, C.; Stöger, B.; Puchberger, M.; Veiros, L. F.; Kirchner, K. *Organometallics* **2013**, *32*, 4114−4121.
(45) Knölker, H.-J.; Heber, J. *Synlett* **1993**, *1993*, 924−926.
(46) Knölker, H.-J.; Heber, J.; Mahler, C. H. *Synlett* **1992**, *1992*, 1002−1004.
(47) Casey, C. P.; Guan, H. *J. Am. Chem. Soc.* **2007**, *129*, 5816−5817.
(48) Casey, C. P.; Guan, H. *J. Am. Chem. Soc.* **2009**, *131*, 2499−2507.
(49) Berkessel, A.; Reichau, S.; von der Höh, A.; Leconte, N.; Neudörfl, J.-M. *Organometallics* **2011**, *30*, 3880−3887.
(50) Zhou, S.; Fleischer, S.; Junge, K.; Beller, M. *Angew. Chem., Int. Ed.* **2011**, *50*, 5120−5124.
(51) Fleischer, S.; Werkmeister, S.; Zhou, S.; Junge, K.; Beller, M. *Chem.—Eur. J.* **2012**, *18*, 9005−9010.
(52) Lagaditis, P. O.; Mikhailine, A. A.; Lough, A. J.; Morris, R. H. *Inorg. Chem.* **2010**, *49*, 1094−1102.
(53) Liang, L.-C.; Li, C.-W.; Lee, P.-Y.; Chang, C.-H.; Man Lee, H. *Dalton Trans.* **2011**, *40*, 9004−9011.
(54) Liang, L.-C.; Chien, P.-S.; Lee, P.-Y. *Organometallics* **2008**, *27*, 3082−3093.
(55) Lansing, R. B., Jr.; Goldberg, K. I.; Kemp, R. A. *Dalton Trans.* **2011**, *40*, 8950−8958.
(56) Benito-Garagorri, D.; Alves, L. G.; Puchberger, M.; Mereiter, K.; Veiros, L. F.; Calhorda, M. J.; Carvalho, M. D.; Ferreira, L. P.; Godinho, M.; Kirchner, K. *Organometallics* **2009**, *28*, 6902−6914.
(57) Benito-Garagorri, D.; Puchberger, M.; Mereiter, K.; Kirchner, K. *Angew. Chem., Int. Ed.* **2008**, *47*, 9142−9145.
(58) Benito-Garagorri, D.; Wiedermann, J.; Pollak, M.; Mereiter, K.; Kirchner, K. *Organometallics* **2007**, *26*, 217−222.
(59) Benito-Garagorri, D.; Alves, L. G.; Veiros, L. F.; Standfest-Hauser, C. M.; Tanaka, S.; Mereiter, K.; Kirchner, K. *Organometallics* **2010**, *29*, 4932−4942.
(60) Antberg, M.; Frosin, K. M.; Dahlenburg, L. *J. Organomet. Chem.* **1988**, *338*, 319−327.
(61) Antberg, M.; Dahlenburg, L. *Z. Naturforsch., B: Chem. Sci.* **1985**, *40*, 1485−1489.
(62) Roger, C.; Marseille, P.; Salus, C.; Hamon, J.-R.; Lapinte, C. *J. Organomet. Chem.* **1987**, *336*, C13−C16.
(63) Field, L. D.; Messerle, B. A.; Smernik, R. J.; Hambley, T. W.; Turner, P. *Inorg. Chem.* **1997**, *36*, 2884−2892.
(64) Liu, T.; Chen, S.; O'Hagan, M. J.; Rakowski DuBois, M.; Bullock, R. M.; DuBois, D. L. *J. Am. Chem. Soc.* **2012**, *134*, 6257−6272.
(65) Gao, Y.; Holah, D. G.; Hughes, A. N.; Spivak, G. J.; Havighurst, M. D.; Magnuson, V. R.; Polyakov, V. *Polyhedron* **1997**, *16*, 2797−2807.
(66) Ohki, Y.; Suzuki, H. *Angew. Chem., Int. Ed.* **2000**, *39*, 3120−3122.
(67) Argouarch, G.; Hamon, P.; Toupet, L.; Hamon, J.-R.; Lapinte, C. *Organometallics* **2002**, *21*, 1341−1348.
(68) Sellmann, D.; Weber, W. *J. Organomet. Chem.* **1986**, *304*, 195−201.
(69) Jia, G.; Drouin, S. D.; Jessop, P. G.; Lough, A. J.; Morris, R. H. *Organometallics* **1993**, *12*, 906−916.
(70) Fiedler, A.; Schröder, D.; Schwarz, H.; Tjelta, B. L.; Armentrout, P. B. *J. Am. Chem. Soc.* **1996**, *118*, 5047−5055.
(71) Noyori, R.; Ohkuma, T. *Angew. Chem., Int. Ed.* **2001**, *40*, 40−73.
(72) Abdur-Rashid, K.; Faatz, M.; Lough, A. J.; Morris, R. H. *J. Am. Chem. Soc.* **2001**, *123*, 7473−7474.
(73) Clapham, S. E.; Hadzovic, A.; Morris, R. H. *Coord. Chem. Rev.* **2004**, *248*, 2201−2237.
(74) Brookhart, M.; Nelson, G. O. *J. Organomet. Chem.* **1979**, *164*, 193−202.
(75) Moulton, B. E.; Duhme-Klair, A. K.; Fairlamb, I. J. S.; Lynam, J. M.; Whitwood, A. C. *Organometallics* **2007**, *26*, 6354−6365.
(76) Knölker, H.-J. *Chem. Rev.* **2000**, *100*, 2941−2962.
(77) Russell, S. K.; Milsmann, C.; Lobkovsky, E.; Weyhermuller, T.; Chirik, P. J. *Inorg. Chem.* **2011**, *50*, 3159−3169.
(78) Luo, L.; Nolan, S. P. *Organometallics* **1992**, *11*, 3483−3486.
(79) Ares, J. R.; Aguey-Zinsou, K. F.; Porcu, M.; Sykes, J. M.; Dornheim, M.; Klassen, T.; Bormann, R. *Mater. Res. Bull.* **2008**, *43*, 1263−1275.
(80) Luo, B.; Kucera, B. E.; Gladfelter, W. L. *Dalton Trans.* **2006**, *0*, 4491−4498.
(81) Clapham, S. E.; Guo, R.; Iuliis, M. Z.-D.; Rasool, N.; Lough, A.; Morris, R. H. *Organometallics* **2006**, *25*, 5477−5486.
(82) Baratta, W.; Ballico, M.; Esposito, G.; Rigo, P. *Chem.—Eur. J.* **2008**, *14*, 5588−5595.
(83) Zhang, J.; Gandelman, M.; Shimon, L. J. W.; Rozenberg, H.; Milstein, D. *Organometallics* **2004**, *23*, 4026−4033.
(84) Kloek, S. M.; Heinekey, D. M.; Goldberg, K. I. *Organometallics* **2006**, *25*, 3007−3011.
(85) Trovitch, R. J.; Lobkovsky, E.; Chirik, P. J. *Inorg. Chem.* **2006**, *45*, 7252−7260.
(86) Mikhailine, A. A.; Lagaditis, P. O.; Sues, P. E.; Lough, A. J.; Morris, R. H. *J. Organomet. Chem.* **2010**, *695*, 1824−1830.

(87) Turrell, P. J.; Wright, J. A.; Peck, J. N. T.; Oganesyan, V. S.; Pickett, C. J. *Angew. Chem., Int. Ed.* **2010**, *49*, 7508−7511.
(88) Marcó, A.; Compano, R.; Rubio, R.; Casals, I. *Microchim. Acta* **2003**, *142*, 13−19.
(89) Frisch, M. J. et al. *Gaussian 2009*, Revision B.2001; Gaussian Inc.: Wallingford CT, 2009.
(90) Zhao, Y.; Truhlar, D. *Theor. Chem. Acc.* **2008**, *120*, 215−241.
(91) Zhao, Y.; Truhlar, D. G. *Acc. Chem. Res.* **2008**, *41*, 157−167.
(92) Marenich, A. V.; Cramer, C. J.; Truhlar, D. G. *J. Phys. Chem. B* **2009**, *113*, 6378−6396.
(93) *GAMESS*, The General Atomic and Molecular Electronic Structure System; http://www.msg.chem.iastate.edu/GAMESS/GAMESS.html.
(94) Schmidt, M. W.; Baldridge, K. K.; Boatz, J. A.; Elbert, S. T.; Gordon, M. S.; Jensen, J. H.; Koseki, S.; Matsunaga, N.; Nguyen, K. A.; Su, S. J.; Windus, T. L.; Dupuis, M.; Montgomery, J. A. *J. Comput. Chem.* **1993**, *14*, 1347.
(95) Hay, P. J.; Wadt, W. R. *J. Chem. Phys.* **1985**, *82*, 270. 284. 299.